

Elements of Propulsion: Gas Turbines and Rockets

Jack D. Mattingly

Professor Emeritus

Department of Mechanical Engineering
Seattle University, Seattle, Washington

Foreword by

Hans von Ohain

German Inventor of the Jet Engine



EDUCATION SERIES

Joseph A. Schetz

Series Editor-in-Chief

Virginia Polytechnic Institute and State University
Blacksburg, Virginia

Published by the
American Institute of Aeronautics and Astronautics, Inc.
1801 Alexander Bell Drive, Reston, Virginia 20191-4344

$$\beta_{1h} = \tan^{-1} \frac{v_{1Rh}}{u_1} = 44.6 \text{ deg}$$

$$\beta_{1t} = \tan^{-1} \frac{v_{1Rt}}{u_1} = 63.1 \text{ deg}$$

$$T_{t3} = T_{t2} = T_{t1} + \frac{\varepsilon U_t^2}{g_c c_p} = 288.16 + \frac{0.9 \times 436.8^2}{1004} = 459.19 \text{ K}$$

$$\eta_c = \frac{(P_{t3}/P_{t1})^{\gamma/(\gamma-1)} - 1}{T_{t3}/T_{t1} - 1} = \frac{4^{1/3.5} - 1}{459.19/288.16 - 1} = 81.9\%$$

$$v_2 = \varepsilon U_t = 0.9 \times 436.8 = 393.1 \text{ m/s}$$

$$w_2 = u_1 = 132.8 \text{ m/s}$$

$$V_2 = \sqrt{w_2^2 + v_2^2} = \sqrt{132.8^2 + 393.1^2} = 414.9 \text{ m/s}$$

$$\alpha_2 = \tan^{-1} \frac{w_2}{v_2} = 18.67 \text{ deg}$$

$$M_2 = \sqrt{\frac{2}{\gamma-1} \left[\frac{T_{t2}}{T_{t2} - V_2^2/(2g_c c_p)} - 1 \right]}$$

$$= \sqrt{5 \left(\frac{459.19}{459.19 - 85.73} - 1 \right)} = 1.071$$

$$\frac{P_{t3s}}{P_{t1}} = \left(\frac{T_{t3}}{T_{t1}} \right)^{\gamma/(\gamma-1)} = 5.108$$

$$\frac{P_{t2}}{P_{t3s}} = \frac{P_{t3}}{P_{t2}} = \sqrt{\frac{P_{t3}/P_{t1}}{P_{t3s}/P_{t1}}} = 0.8849$$

$$P_{t2} = 0.8849 \times 5.108 \times 101.3 = 457.9 \text{ kPa}$$

$$P_{t3} = 4.0 \times 101.3 = 405.2 \text{ kPa}$$

$$\text{MFP}(M_2) = 0.040326$$

$$A_2 = \frac{\dot{m} \sqrt{T_{t2}}}{P_{t2} \text{MFP}(M_2) (\cos \alpha_2)} = \frac{8 \sqrt{459.19}}{457,900 \times 0.040326 \times 0.9474} = 0.0098 \text{ m}^2$$

$$b = \frac{A_2}{\pi d_2} = \frac{0.0098}{\pi \times 0.5} = 0.624 \text{ cm}$$

Table 9.11 Results for Example 9.8 centrifugal compressor

Property	Station				
	1	1R	2R	2	3
T_t K	288.16	296.70/322.36 (hub/tip)	383.23	459.19	459.19
T K	279.37	279.37	272.50	373.50	455.16
P_t kPa	101.3	112.2/150.0	243.1	457.9	405.2
P kPa	90.9	90.9	222.2	222.2	392.9
M	0.3966	0.557/0.877	0.361	1.071	0.2105
V m/s	132.8	186.54/293.82	139.8	414.9	90
u/w m/s	132.8	132.8	132.8	132.8	
v m/s	0	131.0/262.1	43.7	393.1	
r cm		15/30	50.0	50.0	
α deg	0	—	—	18.67	
β deg	—	44.6/63.1	69.1	—	

$$M_3 = \sqrt{\frac{2}{\gamma-1} \left[\frac{T_{t3}}{T_{t3} - V_3^2/(2g_c c_p)} - 1 \right]} \\ = \sqrt{5 \left(\frac{459.19}{459.19 - 4.034} - 1 \right)} = 0.2105$$

$$\text{MFP}(M_3) = 0.014343$$

$$A_3 \cos \alpha_3 = \frac{\dot{m} \sqrt{T_{t3}}}{P_{t3} \text{MFP}(M_3)} = \frac{8 \sqrt{459.19}}{405,200 \times 0.014343} = 0.0295 \text{ m}^2$$

The results of this example are summarized in Table 9.11. Note that different values of flow properties are listed for the hub and tip at station 1R and that M_2 is supersonic while M_{2R} is subsonic.

9.5 Axial-Flow Turbine Analysis

The mass flow of a gas turbine engine, which is limited by the maximum permissible Mach number entering the compressor, is generally large enough to require an axial turbine (even for centrifugal compressors). The axial turbine is essentially the reverse of the axial compressor except for one essential difference: the turbine flow operates under a favorable pressure gradient. This permits greater angular changes, greater pressure changes, greater energy changes, and higher efficiency. However, there is more blade stress involved because of the higher work and temperatures. *It is this latter fact that generally dictates the blade shape.*

Conceptually, a turbine is a very simple device because it is fundamentally no different from a pinwheel that spins rapidly when air is blown against it. The pinwheel will turn in one direction or the other, depending on the direction of the impinging air, and a direction can be found for the air that causes no rotation at all. Thus it is important to properly direct the airstream if the desired motion and speed are to be obtained.

A modern turbine is merely an extension of these basic concepts. Considerable care is taken to establish a directed flow of fluid of high velocity by means of stator blades, and then similar care is used in designing the blades on the rotating wheel (the vanes on the pinwheel) so that the fluid applies the required force to these rotor blades most efficiently. Conceptually, the turbine is a cousin to the pinwheel, but such an analogy gives no appreciation for the source of the tremendous power outputs that can be obtained in a modern turbine. The appreciation comes when one witnesses a static test of the stator blades that direct a gas stream to the rotor of a modern aircraft gas turbine. Such a stream exhausting into the quiescent air of a room will literally rip the paint off the wall at a point 6 ft away in line with the jet direction. When blades of the rotating element are pictured in place immediately at the exit of these directing blades, it then becomes difficult to imagine that the rotor could be constrained from turning and producing power.

Terminology can be a problem in the general field of turbomachinery. Compressor development grew out of aerodynamics and aircraft wing technology, while turbines have historically been associated with the mechanical engineers who developed the steam turbine. The symbols as well as the names used in these two fields differ, but for consistency and to minimize problems for the reader, the turbine will be presented using the nomenclature already established in the beginning of this chapter. Where a term or symbol is in such common use that to ignore it would mean an incomplete education, it will be indicated as an alternate. Thus turbine stator blades are usually called *nozzles* and rotor blades are *buckets*.

In the gas turbine, the high-pressure, high-temperature gas from the combustion chamber flows in an annular space to the stationary blades (called *stators*, *vanes*, or *nozzles*) and is directed tangentially against the rotating blade row (called *rotor blades* or *buckets*). A simple single-stage turbine configuration with nomenclature is shown in Fig. 9.48a. It is convenient to "cut" the blading on a cylindrical surface and look at the section of the stator and rotor blades in two dimensions. This leads to the construction of a vector or velocity diagram for the stage (see Fig. 9.48a) that shows the magnitude and direction of the gas velocities within the stage on the cylindrical surface.

In the stator or nozzle, the fluid is accelerated while the static pressure decreases and the tangential velocity of the fluid is increased in the direction of rotation. The *rotor* decreases the tangential velocity in the direction of rotation, tangential forces are exerted by the fluid on the rotor blades, and a resulting torque is produced on the output shaft. The absolute velocity of the fluid is reduced across the rotor. Relative to the moving blades, typically there is acceleration of the fluid with the associated decrease in static pressure and static temperature. A multistage turbine is made up of consecutive stages, each stage consisting of first a nozzle row followed by a rotor row. Figure 9.48b shows an

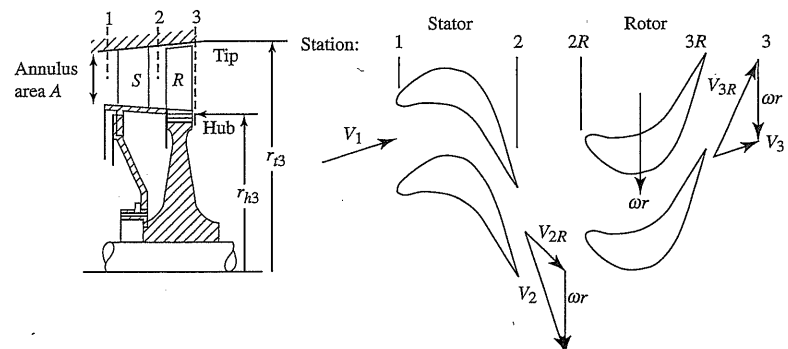


Fig. 9.48a Typical single-stage turbine and velocity diagram.

isometric section of the four-stage turbine for a two-spool, low-bypass-ratio turbofan engine.

The following analysis of the axial-flow turbine stage is performed along the mean radius with radial variations being considered. In many axial-flow turbines, the hub and tip diameters vary little through a stage, and the hub/tip ratio approaches unity. There can be no large radial components of velocity between the annular walls in such stages, there is little variation in static pressure from root to tip, and the flow conditions are little different at each radius.

For these stages of high hub/tip ratio, the two-dimensional analysis is sufficiently accurate. The flow velocity triangles are drawn for the mean-radius

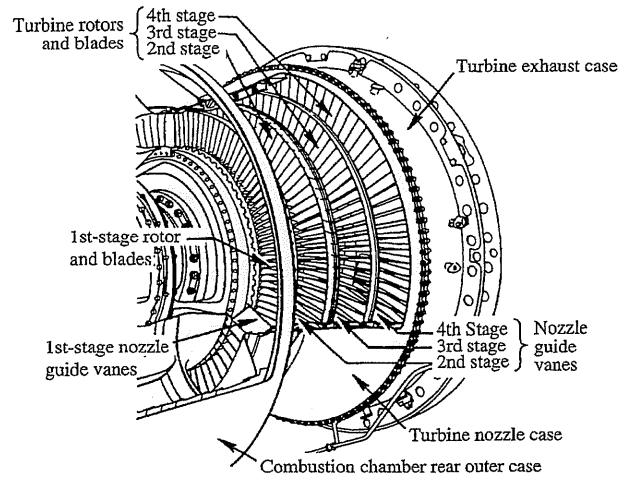


Fig. 9.48b Isometric section of multistage turbine. (Courtesy of Pratt & Whitney.)

condition, but these triangles are assumed to be valid for the other radial sections. The mean-radius analysis presented in this section applies to the total flow for such *two-dimensional* stages: the flow velocity, blade speed, and pressures being assumed constant along the blade length.

From the Euler turbine equation, [Eq. (9.4)], the energy per unit mass flow exchanged between fluid and rotor for $r_2 = r_3$ is

$$h_{t2} - h_{t3} = c_p(T_{t2} - T_{t3}) = \frac{\omega r}{g_c}(v_2 + v_3) \quad (9.74)$$

Inspection of the velocity triangles (Fig. 9.49) shows that because of the large angle α_2 at the stator exit and the large turning possible in the rotor, the value of v_3 is often positive (positive α_3). As a result, the two swirl velocity terms on the right side of Eq. (9.74) add, giving large power output.

The large turning in stator and rotor is possible because, usually, the flow is accelerating through each blade row, that is, $v_2 > v_1$ and $v_{3R} > v_{2R}$. This means that the static pressure drops across both stator and rotor and, under such circumstances, a favorable pressure gradient exists for the boundary layers on the blade and wall surfaces, and separation can be avoided. Accelerating flow is an inherent feature of turbines and means that no general flow breakdown similar to compressor stall will occur.

Note that the vector diagram establishes the characteristics of a stage, and geometrically similar diagrams have the same characteristics. The angles of the vector diagram determine its shape and, therefore, become important design parameters. The velocity magnitudes are not important as performance parameters except in relation to the sonic velocity, i.e., except in terms of the Mach number. The angles may be used directly as design parameters or may be implied through the use of velocity ratios. Thus the magnitude of, say,

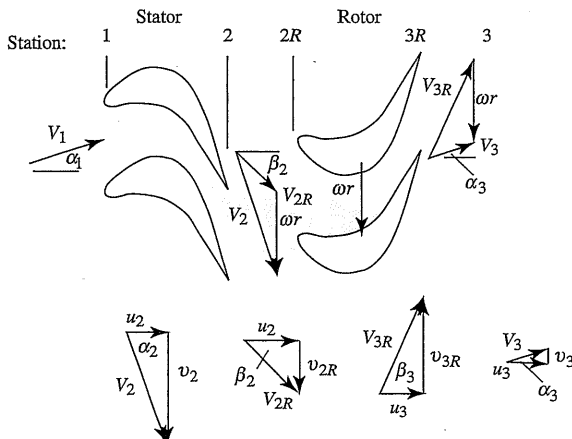


Fig. 9.49 Velocity triangles for a typical turbine stage.

$v_2 + v_3 = \Delta v$, although proportional to the absolute output, is not significant in defining the vector diagram, whereas the ratio $\Delta v/(\omega r)$ helps establish the vector diagram angles and, therefore, the stage characteristics.

The stage analysis in the following sections neglects the influence of cooling air. Thus the flow through the turbine nozzle is assumed to be adiabatic ($T_{t2} = T_{t1}$), as is the flow through the rotor in the relative reference frame ($T_{t3R} = T_{t2R}$). Turbine cooling is discussed at the end of this chapter.

Example 9.9

Consider mean-radius stage calculation—isentropic flow.

Given:

$$T_{t1} = 3200^{\circ}\text{R}, \quad P_{t1} = 300 \text{ psia}, \quad \alpha_2 = 60 \text{ deg}$$

$$\alpha_3 = 0 \text{ deg}, \quad M_2 = 1.1, \quad \omega r = 1400 \text{ ft/s}$$

$$u_3 = u_2, \quad \gamma = 1.3, \quad R = 53.40 \text{ ft} \cdot \text{lbf}/(\text{lbfm} \cdot ^{\circ}\text{R})$$

Find the flow properties for this isentropic turbine stage.

Solution:

$$T_{t2} = T_{t1} = 3200^{\circ}\text{R}$$

$$T_2 = \frac{T_{t2}}{1 + [(\gamma - 1)/2]M_2^2} = \frac{3200}{1 + 0.15 \times 1.1^2} = 2708.4^{\circ}\text{R}$$

$$g_c c_p = g_c \left(\frac{\gamma}{\gamma - 1} \right) R = 32.174 \left(\frac{1.3}{0.3} \right) 53.40 = 7445 \text{ ft}^2/(\text{s}^2 \cdot ^{\circ}\text{R})$$

$$V_2 = \sqrt{2g_c c_p(T_{t2} - T_2)} = \sqrt{2(7445)(3200 - 2708.4)} = 2705.5 \text{ ft/s}$$

$$u_2 = V_2 \cos \alpha_2 = 2705.5 \cos 60 \text{ deg} = 1352.8 \text{ ft/s}$$

$$v_2 = V_2 \sin \alpha_2 = 2705.5 \sin 60 \text{ deg} = 2343.0 \text{ ft/s}$$

$$v_{2R} = v_2 - \omega r = 2343.0 - 1400 = 943.0 \text{ ft/s}$$

$$V_{2R} = \sqrt{u_2^2 + v_{2R}^2} = \sqrt{1352.8^2 + 943.0^2} = 1649.0 \text{ ft/s}$$

$$\beta_2 = \tan^{-1} \frac{v_{2R}}{u_2} = \tan^{-1} \frac{943.0}{1352.8} = 34.88 \text{ deg}$$

$$M_{2R} = M_2 \frac{V_{2R}}{V_2} = 1.1 \left(\frac{1649.0}{2705.5} \right) = 0.670$$

$$T_{t2R} = T_2 + \frac{V_{2R}^2}{2g_c c_p} = 2708.4 + \frac{1649.0^2}{2(7445)} = 2891.0^{\circ}\text{R}$$

$$v_3 = 0$$

$$V_3 = u_3 = u_2 = 1352.8 \text{ ft/s}$$

$$v_{3R} = v_3 + \omega r = 0 + 1400 = 1400 \text{ ft/s}$$

$$V_{3R} = \sqrt{u_3^2 + v_{3R}^2} = \sqrt{1352.8^2 + 1400^2} = 1946.8 \text{ ft/s}$$

$$\beta_3 = \tan^{-1} \frac{v_{3R}}{u_3} = \tan^{-1} \frac{1400}{1352.8} = 45.98 \text{ deg}$$

$$T_{13} = T_{t2} - \frac{\omega r}{g_c c_p} (v_2 + v_3) = 3200 - \frac{1400}{7445} (2343.0 + 0) = 2759.4^\circ\text{R}$$

$$T_3 = T_{13} - \frac{V_3^2}{2g_c c_p} = 2759.4 - \frac{1352.8^2}{2(7445)} = 2636.5^\circ\text{R}$$

$$M_3 = \sqrt{\frac{2}{\gamma - 1} \left(\frac{T_{13}}{T_3} - 1 \right)} = \sqrt{\frac{2}{0.3} \left(\frac{2759.8}{2636.5} - 1 \right)} = 0.558$$

$$M_{3R} = M_3 \frac{V_{3R}}{V_3} = 0.558 \left(\frac{1946.8}{1352.8} \right) = 0.803$$

$$T_{13R} = T_{t2R} = 2891.0^\circ\text{R}$$

$$P_{t2} = P_{t1} = 300 \text{ psia}$$

$$P_2 = P_{t2} \left(\frac{T_2}{T_{t2}} \right)^{\gamma/(\gamma-1)} = 300 \left(\frac{2708.4}{3200} \right)^{1.3/0.3} = 145.6 \text{ psia}$$

$$P_{t2R} = P_2 \left(\frac{T_{t2R}}{T_2} \right)^{\gamma/(\gamma-1)} = 145.6 \left(\frac{2891.0}{2708.4} \right)^{1.3/0.3} = 193.2 \text{ psia}$$

$$P_{13R} = P_{t2R} = 193.2 \text{ psia}$$

$$P_{13} = P_{t2} \left(\frac{T_{13}}{T_{t2}} \right)^{\gamma/(\gamma-1)} = 300 \left(\frac{2759.4}{3200} \right)^{1.3/0.3} = 157.9 \text{ psia}$$

$$P_3 = P_{t2} \left(\frac{T_3}{T_{t2}} \right)^{\gamma/(\gamma-1)} = 157.9 \left(\frac{2636.5}{2759.4} \right)^{1.3/0.3} = 129.6 \text{ psia}$$

Table 9.12 is a summary of the results for this axial-flow turbine stage with isentropic flow. The given data are listed in boldface type. Even though the flow leaving the nozzle (station 2) is supersonic, the relative flow entering the rotor is subsonic. The flow through the rotor is turned 80.8 deg. Figure 9.50 shows the change in temperature and pressure for an isentropic turbine stage.

9.5.1 Stage Parameters

9.5.1.1 Adiabatic efficiency. The adiabatic efficiency (the most common definition of efficiency for turbines) is the ratio of the actual energy output to the

Table 9.12 Results for Example 9.9 axial-flow turbine stage calculation, isentropic flow

Property	Station				
	1	2	2R	3R	3
T_t °R (K)	3200 (1778)	3200.0 (1777.8)	2891.0 (1606.1)	2891.0 (1606.1)	2759.4 (1533.0)
T °R (K)		2708.4 (1504.7)	2708.4 (1504.7)	2636.5 (1464.7)	2636.5 (1464.7)
P_t psia (kPa)	300 (2068)	300 (2068)	193.2 (1332)	193.2 (1332)	157.9 (1089)
P psia (kPa)		145.6 (1004)	145.6 (1004)	129.6 (893.6)	129.6 (893.6)
M	1.10		0.670 (412.3)	0.803 (412.3)	0.558 (412.3)
V ft/s (m/s)		2705.5 (824.6)	1649.0 (502.6)	1946.8 (593.4)	1352.8 (412.3)
u ft/s (m/s)		1352.8 (412.3)	1352.8 (412.3)	1352.8 (412.3)	1352.8 (412.3)
v ft/s (m/s)		2343.0 (714.2)	943.0 (287.4)	1400.0 (426.7)	0 (0)
α deg	60.0				0
β deg			34.88	45.98	

theoretical isentropic output (see Fig. 9.51a) for the same input total state and same exit total pressure:

$$\eta_t = \frac{\text{actual } \Delta h_t}{\text{ideal } \Delta h_t} = \frac{h_{t1} - h_{t3}}{h_{t1} - h_{t3s}} \quad (9.75)$$

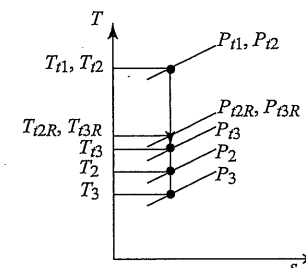


Fig. 9.50 Property changes of an isentropic turbine stage.

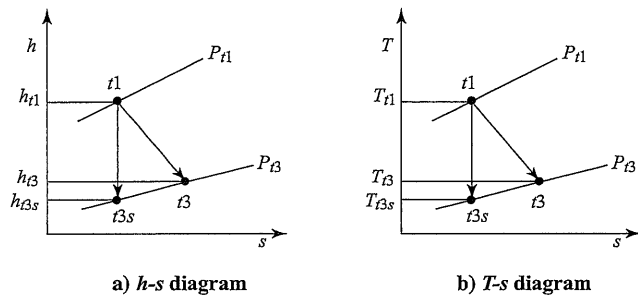


Fig. 9.51 Definition of turbine adiabatic efficiency.

For a calorically perfect gas, the efficiency can be written in terms of total temperatures and total pressures (see Fig. 9.51b) as follows:

$$\eta_t = \frac{h_{t1} - h_{t3}}{h_{t1} - h_{\beta s}} = \frac{c_p(T_{t1} - T_{\beta s})}{c_p(T_{t1} - T_{\beta s})}$$

$$\eta_t = \frac{1 - T_{\beta s}/T_{t1}}{1 - (P_{\beta s}/P_{t1})^{(\gamma-1)/\gamma}} \quad (9.6)$$

The preceding definition is sometimes called the *total-to-total turbine efficiency* η_t , since the theoretical output is based on the leaving total pressure.

9.5.1.2 Exit swirl angle. The absolute angle of the leaving flow α_3 is called the *swirl angle* and, by convention, is positive when opposite to wheel speed direction (*backward-running*). The angle is important for two reasons. It is difficult in any fluid dynamic situation to efficiently convert kinetic energy to pressure or potential energy, and the kinetic energy in the flow leaving a turbine stage can be minimized by having $v_3 = u_3$, that is, by having zero swirl. Conversely, we see that the higher the swirl angle (if backward-running), the higher in magnitude v_3 will be, which generally means higher output from the stage [see Eq. (9.74) and Fig. 9.49].

9.5.1.3 Stage loading and flow coefficients. The *stage loading coefficient*, defined by Eq. (9.19), is the ratio of the stage work per unit mass to the rotor speed squared, or

$$\psi = \frac{g_c \Delta h_t}{(\omega r)^2} = \frac{g_c \Delta h_t}{U^2}$$

For a calorically perfect gas, we write [Eq. (9.20)]

$$\psi = \frac{g_c c_p \Delta T_t}{(\omega r)^2} = \frac{g_c c_p \Delta T_t}{U^2}$$

The ratio of the axial velocity entering the rotor to the rotor speed is called the *flow coefficient* and is defined as

$$\Phi = \frac{u_2}{\omega r} = \frac{u_2}{U} \quad (9.77)$$

The stage loading coefficient and flow coefficient for a turbine stage have a range of values. Figure 9.52 shows the range of these coefficients for several types of turbines. For Example 9.9 data, the stage loading coefficient is 1.67, and the flow coefficient is 0.962, which is well within the range for high-efficiency axial-flow turbines. Both the stage loading and flow coefficients affect the turbine stage efficiency, as shown in Fig. 9.53. Modern high-pressure turbines used for aircraft gas turbine engines have stage loading coefficients in the range of 1.3–2.2 and flow coefficients in the range of 0.5–1.1.

From Fig. 9.49 and Eqs. (9.74), (9.20), and (9.77), we obtain the stage loading coefficient in terms of the flow coefficient, the axial velocity ratio u_3/u_2 , and flow angles as

$$\psi = \frac{g_c c_p \Delta T}{(\omega r)^2} = \frac{v_2 + v_3}{\omega r} = \Phi \left(\tan \alpha_2 + \frac{u_3}{u_2} \tan \alpha_3 \right) \quad (9.78a)$$

or

$$\psi = \frac{g_c c_p \Delta T}{(\omega r)^2} = \frac{v_2 + v_3}{\omega r} = \Phi \left(\tan \beta_2 + \frac{u_3}{u_2} \tan \beta_3 \right) \quad (9.78b)$$

By using Fig. 9.49, the flow coefficient can be expressed in terms of the flow angles as

$$\Phi = (\tan \alpha_2 - \tan \beta_2)^{-1} \quad (9.79)$$

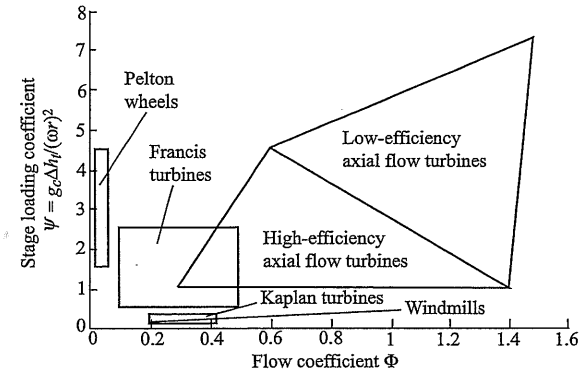


Fig. 9.52 Stage loading vs flow coefficient for different turbine types (Ref. 40).

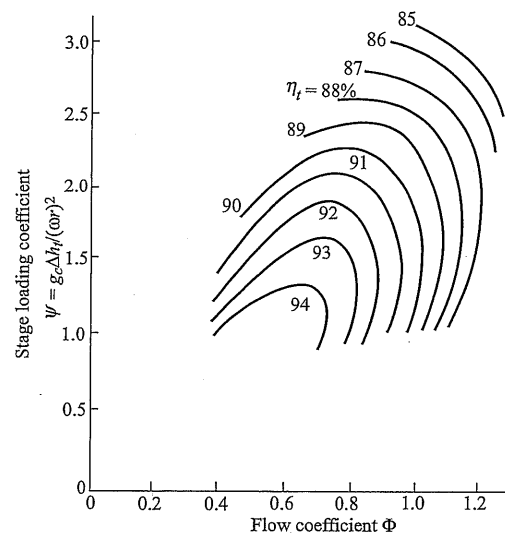


Fig. 9.53 Stage efficiency vs stage loading and flow coefficients, corrected for zero tip leakage (Ref. 40).

We obtain the following expression for the stage loading coefficient in terms of flow angles and u_3/u_2 by combining Eqs. (9.78a) and (9.79):

$$\psi = \frac{\tan \alpha_2 + (u_3/u_2)(\tan \alpha_3)}{\tan \alpha_2 - \tan \beta_2} \quad (9.80)$$

Equations (9.79) and (9.80) are plotted in Fig. 9.54 for constant axial velocity over a range of α_2 and β_2 and specific values of Φ , ψ , and α_3 . This figure shows the effect of changing flow angles on Φ and ψ . Increasing α_3 with α_2 and β_2 held constant increases ψ and decreases Φ . Figure 9.54 also can be used to approximately determine the flow coefficient Φ from flow angles α_2 and β_2 and/or the stage loading coefficient ψ from flow angles α_2 , β_2 , and α_3 . For example, given $\alpha_2 = 65^\circ$, $\beta_2 = 40^\circ$, and $\alpha_3 = 10^\circ$, Fig. 9.49 gives Φ of about 0.77 and ψ of about 1.8. More accurate results can be obtained by using Eqs. (9.79) and (9.80).

Figure 9.55 shows the rotor turning ($\varepsilon = \beta_2 + \beta_3$) for constant axial velocity as a function of the flow angle β_2 for different values of the ratio ψ/Φ . This figure can be used in conjunction with Fig. 9.54 to determine the rotor turning ε and the flow angle β_3 .

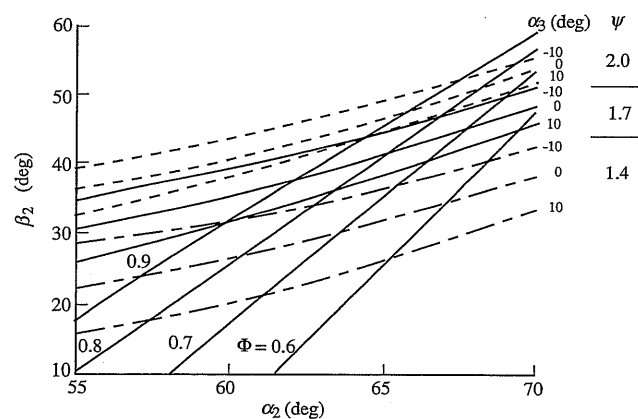


Fig. 9.54 Stage loading and flow coefficients vs flow angles (constant axial velocity).

9.5.1.4 Degree of reaction. The *degree of reaction* is defined as

$$^{\circ}R_t = \frac{h_2 - h_3}{h_{t1} - h_{t3}} \quad (9.81a)$$

For a calorically perfect gas, we can write

$$^{\circ}R_t = \frac{T_2 - T_3}{T_{t1} - T_{t3}} \quad (9.81b)$$

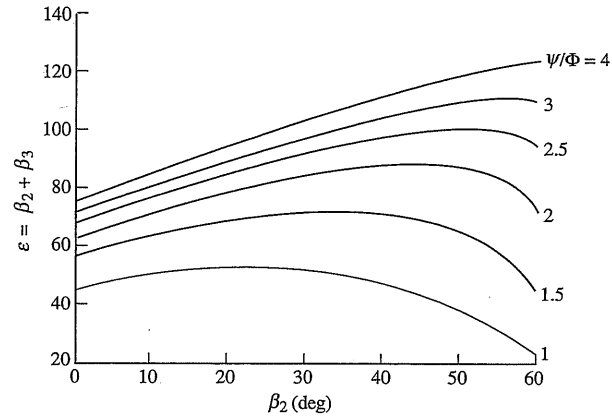
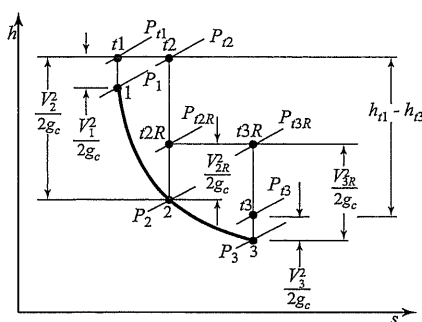


Fig. 9.55 Rotor turning ε vs Ψ/Φ and β_2 (constant axial velocity).

Fig. 9.56 The h - s diagram for general turbine stage.

That is, the degree of reaction is the ratio of the static enthalpy drop in the rotor to the drop in total enthalpy across both the rotor and stator. Figure 9.56 gives a complete picture for a general turbine stage. For Example 9.9, the degree of reaction is 0.166.

It can be shown that the degree of reaction may be related to the flow angles for the case of constant axial velocity ($u_3 = u_2$) by

$${}^{\circ}R_t = \frac{u_2 \tan \beta_3 - \tan \beta_2}{\omega r} = \frac{\Phi \tan \beta_3 - \tan \beta_2}{2} \quad (9.82)$$

By using Eq. (9.82), plots of ${}^{\circ}R_t/\Phi$ were added to Fig. 9.55, giving Fig. 9.57. One can see from this figure that zero reaction corresponds to maximum rotor turning ϵ for fixed value of ψ/Φ .

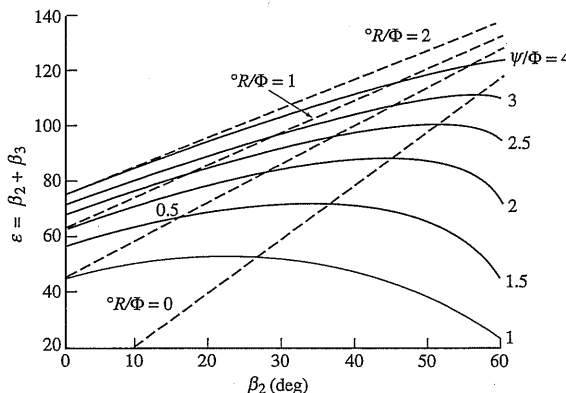


Fig. 9.57 Degree of reaction, stage loading coefficient, and flow coefficient vs rotor flow angles.

Three important basic designs of turbine are related to the choice of reaction—zero reaction, 50% reaction, and axial leaving velocity (variable reaction). It should be emphasized, however, that the designer is not limited to these three types and that in a three-dimensional turbine design, the reaction may vary continuously along the blades.

Zero reaction: From the definition of reaction, if the reaction is selected as zero for the case of constant axial velocity, then

$$h_3 = h_2 \quad \text{and} \quad \tan \beta_3 = \tan \beta_2$$

Therefore,

$$\beta_3 = \beta_2 \quad \text{and} \quad V_{3R} = V_{2R}$$

Velocity triangles for this zero reaction stage are shown in Fig. 9.58a, and the h - s diagram is drawn in Fig. 9.58b.

If the flow is isentropic and the fluid is a perfect gas, then the condition of zero enthalpy drop ($h_3 - h_2 = 0$) implies no change in pressure across the rotor. The turbine is then called an impulse turbine, with the tangential load arising from impulsive forces only. *It is important to note that reaction is defined here not on the basis of pressure drops, but in terms of static enthalpy changes.* Note, however, that there is a pressure drop from P_2 to P_3 across the rotor, and the

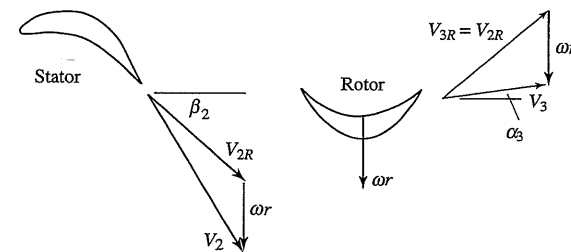
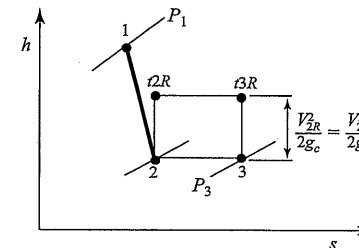
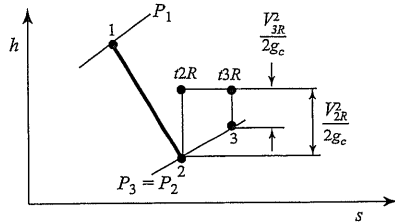


Fig. 9.58a Zero-reaction velocity diagram.

Fig. 9.58b Zero-reaction h - s diagram.

Fig. 9.59 Impulse turbine h - s diagram.

stage is not, therefore, truly impulse. The h - s diagram for an "impulse" stage of zero pressure drop is shown in Fig. 9.59. There is an enthalpy increase from h_2 to h_3 across the rotor, and the relative velocity decreases. Thus, the impulse stage is actually one of negative reaction!

The stage loading coefficient for the impulse stage with constant axial velocity is

$$\psi = \frac{g_c c_p \Delta T_t}{(\omega r)^2} = \frac{\omega r \Delta v}{(\omega r)^2} = \frac{\Delta v}{\omega r}$$

with

$$v_2 = u_2 \tan \alpha_2$$

$$v_3 = u_2 \tan \alpha_3 = u_2 \tan \alpha_2 - 2\omega r$$

then

$$\psi = 2(\Phi \tan \alpha_2 - 1) = 2\Phi \tan \beta_2 \quad (9.83)$$

We desire α_2 to be large. However, this leads to large v_2 and large v_{2R} , which lead to large losses. Thus α_2 is generally limited to less than 70 deg.

Also, if (see Fig. 9.58a) $\alpha_3 = 0$ (no exit swirl), then $\tan \alpha_2 = 2\omega r/u_2$ and

$$\psi = 2 \quad \text{no exit swirl} \quad (9.84)$$

Thus we see that the rotor speed ωr is proportional to $\sqrt{\Delta h_t}$. If the resultant blade speed is too high, we must go to a multistage turbine.

50% reaction: If there is equal enthalpy drop across rotor and stator, then $R_t = 0.5$ and the velocity triangles are symmetrical, as shown in Fig. 9.60. Then, $\alpha_2 = \beta_3$, $\alpha_3 = \beta_2$, and

$$\tan \beta_3 - \tan \beta_2 = \tan \alpha_2 - \tan \alpha_3 = \frac{\omega r}{u_2} = \frac{1}{\Phi}$$

The stage loading coefficient for this turbine with constant axial velocity is

$$\psi = \frac{\Delta v}{\omega r} = 2\Phi \tan \alpha_2 - 1 = 2\Phi \tan \beta_3 - 1 \quad (9.85)$$

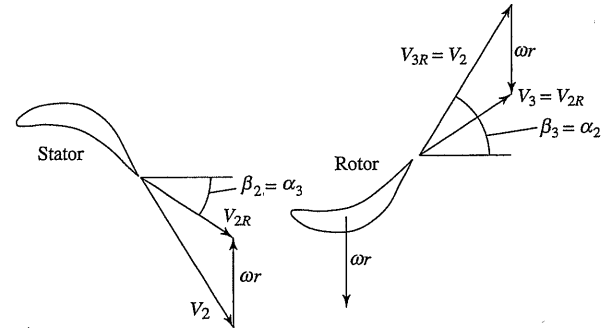


Fig. 9.60 Diagram of 50% reaction turbine velocity.

Again, α_2 should be high but is limited to less than 70 deg. For zero exit swirl

$$\tan \beta_3 = \tan \alpha_2 = \frac{\omega r}{u}, \quad \beta_2 = 0, \quad \psi = 1 \quad (9.86)$$

Thus, for the same ωr and $v_3 = 0$, the work per unit mass from a zero-reaction turbine is twice that from the 50% reaction turbine [compare Eqs. (9.84) and (9.86)].

General zero-swirl case (constant axial velocity): If the exit swirl is to be zero (Fig. 9.61), then $\alpha_3 = 0$, $v_3 = 0$, and $\tan \beta_3 = \omega r/u$. From Eq. (9.82), the reaction is then

$$\begin{aligned} {}^o R_t &= \frac{u}{2\omega r} \left(\frac{\omega r}{u} - \tan \beta_2 \right) = \frac{1}{2} - \frac{u \tan \beta_2}{2\omega r} = 1 - \frac{v_2}{2\omega r} \\ {}^o R_t &= 1 - \frac{v_2}{2\omega r} = 1 - \frac{\psi}{2} \end{aligned} \quad (9.87)$$

This equation can be rewritten as

$$\psi = 2(1 - {}^o R_t) \quad (9.88)$$

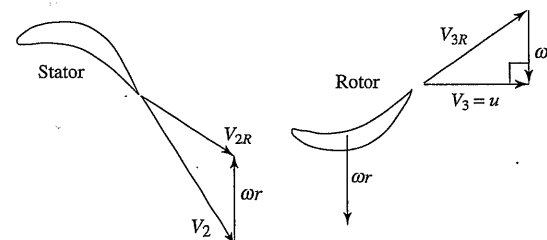


Fig. 9.61 Zero-exit-swirl turbine.

Thus high stage loadings give a low degree of reaction. In aircraft gas turbine engines, engine weight and performance must be balanced. Weight can be reduced by increasing stage loading (reduces the number of turbine stages), but this normally leads to a loss in stage efficiency (see Fig. 9.53).

9.5.1.5 Turbine airfoil nomenclature and design metal angles. The nomenclature for turbine airfoil cascades is presented in Fig. 9.62. The situation in unchoked turbines is similar to that in compressors except that the deviations are markedly smaller because of the thinner boundary layers. Hence

$$\delta_t = \frac{\gamma_i + \gamma_e}{8\sqrt{\sigma}} \quad (9.89)$$

is a good estimate of the turbine exit deviation. More importantly, however, when the turbine airfoil cascade exit Mach number is near unity, the deviation is usually negligible because the cascade passage is similar to a nozzle. In fact, the suction (or convex) surface of the airfoils often has a flat stretch before the trailing edge, which evokes the name *straight-backed*. Finally, the simple concept of deviation loses all meaning at large supersonic exit Mach numbers because expansion or compression waves emanating from the trailing edge can dramatically alter the final flow direction. This is a truly fascinating field of aerodynamics, but one that requires considerable study.

9.5.1.6 Stage temperature ratio τ_s . The stage temperature ratio ($\tau_s = T_{t1}/T_{t3}$) can be expressed as follows, by using the definition of the stage loading coefficient:

$$\tau_s = \frac{T_{t3}}{T_{t1}} = 1 - \psi \frac{(\omega r)^2}{g_c c_p T_{t1}} \quad (9.90)$$

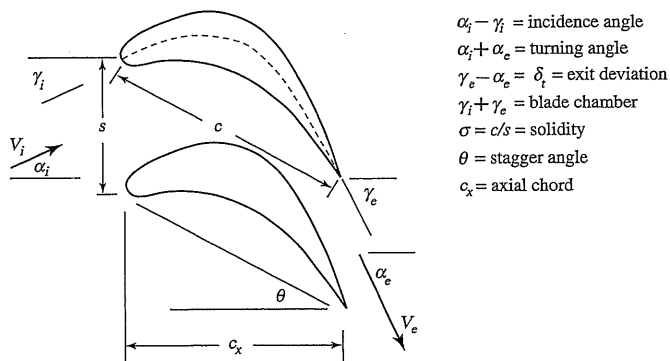


Fig. 9.62 Turbine airfoil nomenclature.

Thus, for a given T_{t1} and ωr , the zero-reaction turbine stage will have the lower stage temperature ratio (greater work output per unit mass) than a 50% reaction turbine stage.

9.5.1.7 Stage pressure ratio π_s . Once the stage temperature ratio, flow-field, and airfoil characteristics are established, several avenues are open to predict the stage pressure ratio. The most simple and direct method is to employ the polytropic efficiency e_t . Recall that the polytropic efficiency is

$$e_t = \frac{dh_t}{dh_{t\text{ideal}}} = \frac{\gamma}{\gamma - 1} \frac{dT_t/T_t}{dP_t/P_t}$$

Integration with constant γ and e_t yields the following equation for the stage pressure ratio

$$\pi_s = \frac{P_{t3}}{P_{t1}} = \left(\frac{T_{t3}}{T_{t1}} \right)^{\gamma/[(\gamma-1)e_t]} = \tau_s^{\gamma/[(\gamma-1)e_t]} \quad (9.91)$$

where the stage temperature ratio can be obtained from the total temperatures or an equation like Eq. (9.90).

Another approach involves the use of experimental or empirical cascade loss correlations, such as those shown in Figs. 9.63 and 9.64, to the stator and rotor in order to determine the total pressure loss. The *total pressure loss coefficient* for turbine cascade data is defined as

$$\phi_t = \frac{P_{ti} - P_{te}}{P_{te} - P_e} \quad (9.92)$$

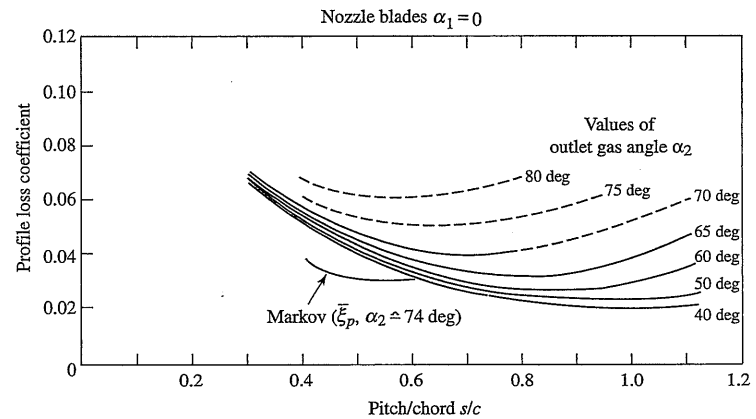


Fig. 9.63 Turbine stator cascade loss coefficient ($\alpha_1 = 0$) (Ref. 40).

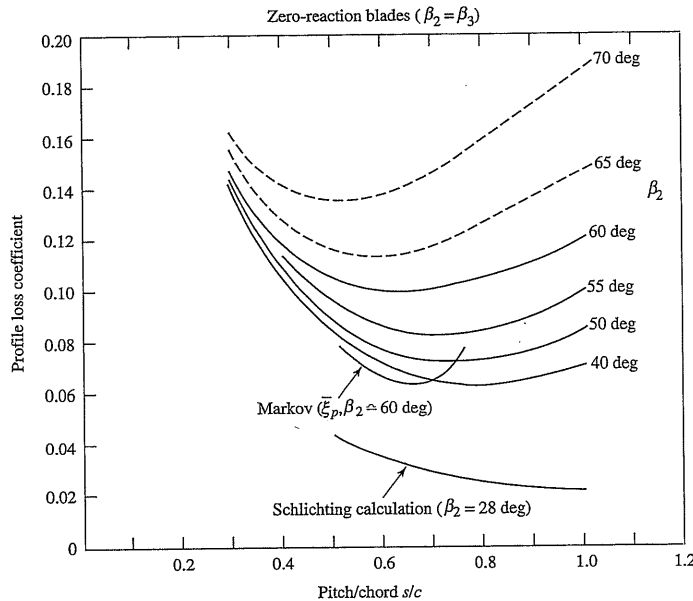


Fig. 9.64 Turbine rotor cascade loss coefficient ($\beta_2 = \beta_3$) (Ref. 40).

where subscripts *i* and *e* refer to the inlet and exit states, respectively. This equation can be rewritten for the cascade total pressure ratio as

$$\frac{P_{te}}{P_{ti}} = \frac{1}{1 + \phi_i(1 - P_e/P_{te})} \quad (9.93)$$

where P_e/P_{te} depends only on the usually known airfoil cascade exit Mach number M_e . Note that the total pressure loss coefficient for the rotor is based on the relative total states. The stage total pressure ratio can be written as

$$\frac{P_{t3}}{P_{t1}} = \left(\frac{P_{t2}}{P_{t1}}\right)_{\phi_t \text{ stator}, M_2} \frac{P_{t2R}}{P_{t2}} \left(\frac{P_{t3R}}{P_{t2R}}\right)_{\phi_t \text{ rotor}, M_{3R}} \frac{P_{t3}}{P_{t3R}} \quad (9.94)$$

where ϕ_t stator and ϕ_t rotor are the loss coefficients for the stator and rotor, respectively, and the subscripted total pressure ratios are obtained from Eq. (9.93) and cascade data. Additional losses are associated with tip leakage, annulus boundary layers, and secondary flows. Then, with all the stator, rotor, and stage properties computed, the stage efficiency can be computed from Eq. (9.76).

9.5.1.8 Blade spacing. The momentum equation relates the tangential force of the blades on the fluid to the change in tangential momentum of the fluid. This force is equal and opposite to that which results from the difference in pressure between the pressure side and the suction side of the airfoil. Figure 9.65 shows the variation in pressure on both the suction and pressure surfaces of a typical turbine airfoil from cascade tests. On the pressure surface, the pressure is nearly equal to the inlet total pressure for 60% of the length before the fluid is accelerated to the exit pressure condition. However, on the suction surface, the fluid is accelerated in the first 60% of the length to a low pressure and then is decelerated to the exit pressure condition. The deceleration on the suction surface is limited and controlled since it can lead to boundary-layer separation.

Enough airfoils must be present in each row that the sum of the tangential force on each is equal to the change in tangential momentum of the fluid. A simple expression for the relationship of the blade spacing to the fluid flow angles is developed in this section based on an incompressible fluid. This same expression correlates to the required blade spacing in a turbine stator or rotor row.

Referring to the cascade nomenclature in Fig. 9.62, we see that the tangential force per unit depth of blades spaced a distance *s* apart is

$$F_t = \frac{\rho u_i s(v_i + v_e)}{g_c} = \frac{\rho u_i^2 s}{g_c} \left(\tan \alpha_i + \frac{u_e}{u_i} \tan \alpha_e \right) \quad (9.95)$$

Zweifel⁵³ defines a tangential force coefficient that is the ratio of the force given by Eq. (9.95) to the maximum tangential force $F_{t \max}$ that can be achieved efficiently, and $F_{t \max}$ is obtained when

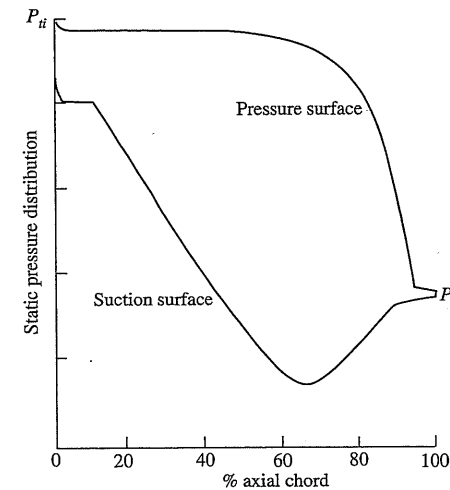


Fig. 9.65 Pressure distribution on a turbine cascade airfoil.

1) The pressure on the pressure surface is maintained at the inlet total pressure and drops to the exit static pressure at the trailing edge.

2) The pressure on the suction surface drops to the exit static pressure at the leading edge and remains at this value.

Thus the maximum tangential force is $F_{t \max} = (P_{ti} - P_e)c_x$, where c_x is the axial chord of the blade (see Fig. 9.62). For reversible flow of an incompressible fluid, $F_{t \max}$ can be written as

$$F_{t \max} = \frac{\rho V_e^2 c_x}{2g_c} = \frac{\rho u_e^2 c_x}{2g_c \cos^2 \alpha_e} \quad (9.96)$$

The Zweifel tangential force coefficient Z is defined as

$$Z = \frac{F_t}{F_{t \max}} \quad (9.97)$$

From Eqs. (9.95) and (9.96), the equation of Z for a cascade airfoil becomes

$$Z = \frac{2s}{c_x} (\cos^2 \alpha_e) \left(\tan \alpha_t + \frac{u_e}{u_i} \tan \alpha_e \right) \left(\frac{u_i}{u_e} \right)^2$$

For the stator, we write

$$Z_s = \frac{2s}{c_x} (\cos^2 \alpha_2) \left(\tan \alpha_1 + \frac{u_2}{u_1} \tan \alpha_2 \right) \left(\frac{u_1}{u_2} \right)^2 \quad (9.98a)$$

Likewise for the rotor, we write

$$Z_r = \frac{2s}{c_x} (\cos^2 \beta_3) \left(\tan \beta_2 + \frac{u_3}{u_2} \tan \beta_3 \right) \left(\frac{u_2}{u_3} \right)^2 \quad (9.98b)$$

Because suction surface pressures can be less than the exit static pressure along the blade (see Fig. 9.65), Z values near unity are attainable. By using Eq. (9.98b), lines of constant $Z_r c_x / s$ are plotted in Fig. 9.66 vs the relative rotor angles β_2 and β_3 . High β_2 and zero reaction (high stage loading ψ , see Fig. 9.57) give high values of $Z_r c_x / s$ (see Fig. 9.66) and require high values of solidity [$\sigma = c/s = (c_x/s)/\cos \theta$]. High solidity at high β_2 and zero reaction can lead to high total pressure losses (see Fig. 9.64). For no exit swirl ($\alpha_3 = 0$), the 50% reaction stage ($\psi = 1$) corresponds to $\beta_2 = 0$, the required solidity is low (Fig. 9.66), and the total pressure losses are low (Fig. 9.64). Thus the turbine design for aircraft engines will be a balance between the number of stages (stage loadings) and the turbine efficiency (total pressure losses).

9.5.1.9 Radial variations. Because the mass flow rate per unit area [that is, $\dot{m}/A = P_t/(MFP\sqrt{T_t})$] is higher in turbines than in compressors, turbine

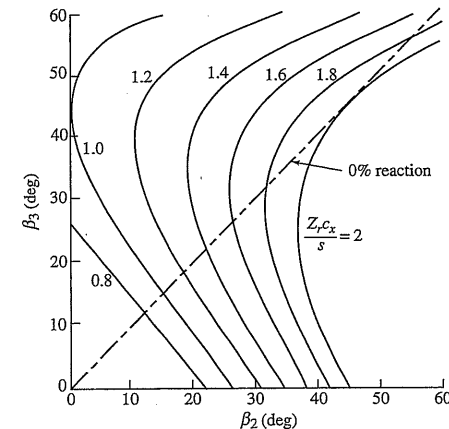


Fig. 9.66 $Z c_x/s$ of rotor vs β_2 and β_3 .

airfoils are correspondingly shorter. The result is little radial variation of aerodynamic properties from hub to tip except in the last few stages of the low-pressure turbine. Figure 9.67 is the rotor blade of a low-pressure turbine that shows radial variation from hub to tip. Typically, the degree of reaction varies from near zero at the hub to about 40% at the tip.

If the aerodynamic design of these stages began as free vortex, the swirl distribution with radius is the same as for compressors, given by [Eq. (9.45)]

$$v = v_m \frac{r_m}{r}$$

For constant axial velocity ($u_2 = u_3$), the degree of reaction is

$$\begin{aligned} {}^\circ R_t &= \frac{T_2 - T_3}{T_{t1} - T_{t3}} = \frac{T_2 - T_3}{T_{t2} - T_{t3}} = 1 - \frac{V_2^2 - V_3^2}{2g_c c_p (T_{t1} - T_{t3})} = 1 - \frac{v_2^2 - v_3^2}{2\omega r(v_2 + v_3)} \\ &= 1 - \frac{v_2 - v_3}{2\omega r} \end{aligned}$$

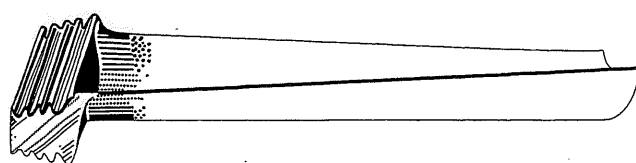


Fig. 9.67 Low-pressure turbine rotor blade. (Courtesy of Pratt & Whitney.)

Substituting Eq. (9.44), we write the degree of reaction at any radius in terms of the degree of reaction at the mean radius as

$$\begin{aligned} \text{°}R_t &= 1 - \frac{v_{m2} - v_{m3} r_m}{2\omega r} = 1 - \frac{v_{m2} - v_{m3}}{2\omega r_m} \left(\frac{r_m}{r} \right)^2 \\ \text{°}R_t &= 1 - (1 - \text{°}R_{tm}) \left(\frac{r_m}{r} \right)^2 \end{aligned} \quad (9.99)$$

This is the same result as for compressors [Eqs. (9.51) and (9.52)]. Consequently, the most difficult airfoil contours to design would be at the hub of the rotating airfoils and at the tips of the stationary airfoils where the degree of reaction is low. It is, therefore, possible to find portions of some airfoils near the rear of highly loaded (i.e., high work per stage), low-pressure turbines where the static pressure actually rises across the cascade and boundary-layer separation is hard to avoid. In these cases, turbine designers have used their computers to develop nonfree or controlled vortex machines without these troublesome regions in order to maintain high efficiency at high loading.

Because of radial variations, the degree of reaction is lowest at the hub. Hence the Zweifel tangential force coefficient of the rotor Z_r times c_x/s will be maximum at the hub. Although the blade spacing varies directly with radius, $Z_r c_x/s$ is greatest at the hub and decreases faster than $1/r$ with increasing radius. Thus the value of $Z_r c_x/s$ at the rotor hub determines the spacing and number of rotor blades. For the stator, $Z_s c_x/s$ will be greatest at the tip, and its value determines the spacing and number of stator blades.

9.5.1.10 Velocity ratio. The *velocity ratio* (VR) is defined as the ratio of the rotor speed ($U = \omega r$) to the velocity equivalent of the change in stage total enthalpy, or

$$\text{VR} \equiv \frac{U}{\sqrt{2g_c \Delta h_t}} = \frac{\omega r}{\sqrt{2g_c \Delta h_t}} \quad (9.100)$$

The velocity ratio is used by some turbine designers rather than the stage loading coefficient ψ , and one can show that

$$\text{VR} = \frac{1}{\sqrt{2\psi}} \quad (9.101)$$

The VR at the mean radius ranges between 0.5 and 0.6 for modern aircraft gas turbine engines. This range corresponds to stage loading coefficients ψ between 1.4 and 2.

9.5.2 Axial-Flow Turbine Stage

Consider the flow through a single-stage turbine as shown in Fig. 9.68. For generality, we will allow the axial velocity to change from station 2 to 3. The

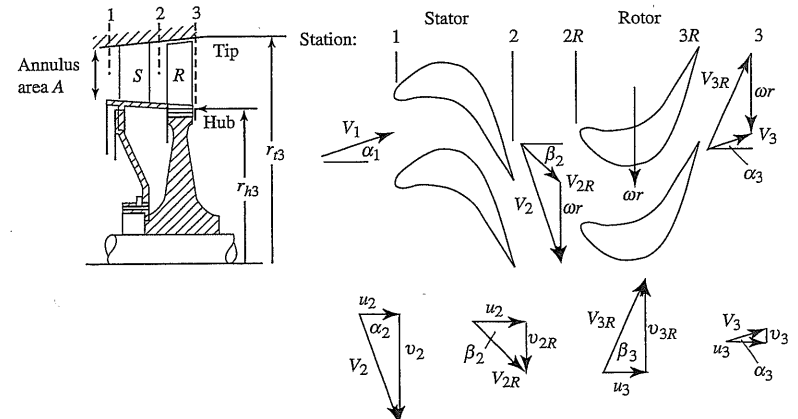


Fig. 9.68 Axial-flow turbine stage (after Ref. 29).

flows through the nozzle (stator) and rotor are assumed to be adiabatic. For solution, we assume that the following data are known: M_2 , T_{t1} , T_{t3} , ωr , α_3 , c_p , γ , and u_3/u_2 . We will develop and write the equations for a general axial-flow turbine based on these known data.

To solve for the flow angle at station 2(α_2), we first write the Euler turbine equation

$$c_p(T_{t2} - T_{t3}) = \frac{\omega r}{g_c} (v_2 + v_3) \quad (9.102)$$

Solving for v_2 , we have

$$v_2 = \frac{g_c c_p \Delta T_t}{\omega r} - v_3$$

Then

$$\sin \alpha_2 = \frac{v_2}{V_2} = \frac{g_c c_p \Delta T_t}{\omega r V_2} - \frac{v_3}{V_2} \quad (i)$$

However,

$$\frac{v_3}{V_2} = \frac{u_3}{V_2} \tan \alpha_3 = \frac{u_3}{u_2} \frac{u_2}{V_2} \tan \alpha_3 = \frac{u_3}{u_2} \cos \alpha_2 \tan \alpha_3$$

Thus, Eq. (i) becomes

$$\sin \alpha_2 = \frac{v_2}{V_2} = \frac{g_c c_p \Delta T_t}{\omega r V_2} - \frac{u_3}{u_2} \cos \alpha_2 \tan \alpha_3 \quad (ii)$$

By using the stage loading parameter ψ , Eq. (ii) can be written as

$$\sin \alpha_2 = \psi \frac{\omega r}{V_2} - \frac{u_3}{u_2} \cos \alpha_2 \tan \alpha_3 \quad (9.103)$$

The velocity at station 2 can be found from

$$V_2 = M_2 a_2 = \sqrt{\frac{2g_c c_p T_{t2}}{1 + 2/[(\gamma - 1)M_2^2]}} \quad (9.104)$$

If $\alpha_3 = 0$, then Eq. (9.103) simplifies to

$$\sin \alpha_2 = \psi \frac{\omega r}{V_2} \quad (9.105)$$

If α_3 is not zero, Eq. (9.103) can be solved by substituting $\sqrt{1 - \sin^2 \alpha_2}$ for $\cos \alpha_2$, squaring both sides of the equation, and solving the resulting quadratic equation for $\sin \alpha_2$. The solution is

$$\sin \alpha_2 = \frac{\left(\psi \frac{\omega r}{V_2}\right) - \left(\frac{u_3}{u_2} \tan \alpha_3\right) \sqrt{1 + \left(\frac{u_3}{u_2} \tan \alpha_3\right)^2 - \left(\psi \frac{\omega r}{V_2}\right)^2}}{1 + \left(\frac{u_3}{u_2} \tan \alpha_3\right)^2} \quad (9.106)$$

The velocity at station 3 can be written in terms of that at station 2 and the two flow angles α_2 and α_3 :

$$V_3 = \frac{u_3 \cos \alpha_2}{u_2 \cos \alpha_3} V_2 \quad (9.107)$$

The degree of reaction can be written in terms of the given data as follows:

$$\begin{aligned} {}^o R_t &= \frac{T_2 - T_3}{T_{t2} - T_{t3}} = \frac{T_{t2} - T_{t3} - (T_{t2} - T_2) + T_{t3} - T_3}{T_{t2} - T_{t3}} \\ &= 1 - \frac{V_2^2 - V_3^2}{2g_c c_p (T_{t2} - T_{t3})} = 1 - \frac{V_2^2 - V_3^2}{2\psi(\omega r)^2} \\ &= 1 - \frac{1}{2\psi(\omega r)^2} \left(\frac{u_2^2}{\cos^2 \alpha_2} - \frac{u_3^2}{\cos^2 \alpha_3} \right) \\ {}^o R_t &= 1 - \frac{1}{2\psi} \left(\frac{V_2}{\omega r} \right)^2 \left[1 - \left(\frac{u_3 \cos \alpha_2}{u_2 \cos \alpha_3} \right)^2 \right] \end{aligned} \quad (9.108)$$

The Mach number at station 3 can be found from

$$M_3 = M_2 \frac{V_3}{V_2} \sqrt{\frac{T_2}{T_3}} \quad (9.109)$$

where

$$\frac{T_3}{T_2} = 1 - {}^o R_t \frac{\Delta T_t}{T_{t2}} \left(1 + \frac{\gamma - 1}{2} M_2^2 \right) \quad (9.110)$$

An equation for the Mach number at station $2R$ can be developed as follows:

$$M_{2R} = M_2 \frac{V_{2R}}{V_2}$$

where

$$V_{2R} = \sqrt{u_2^2 + (v_2 - \omega r)^2} = V_2 \sqrt{\cos^2 \alpha_2 + \left(\sin \alpha_2 - \frac{\omega r}{V_2} \right)^2}$$

Thus

$$M_{2R} = M_2 \sqrt{\cos^2 \alpha_2 + \left(\sin \alpha_2 - \frac{\omega r}{V_2} \right)^2} \quad (9.111)$$

Likewise, an equation for the Mach number at station $3R$ is developed as follows:

$$M_{3R} = M_3 \frac{V_{3R}}{V_3}$$

where

$$V_{3R} = \sqrt{u_3^2 + (v_3 + \omega r)^2} = V_3 \sqrt{\cos^2 \alpha_3 + \left(\sin \alpha_3 + \frac{\omega r}{V_3} \right)^2}$$

Thus

$$M_{3R} = M_3 \sqrt{\cos^2 \alpha_3 + \left(\sin \alpha_3 + \frac{\omega r}{V_3} \right)^2} \quad (9.112)$$

An equation for the rotor relative total temperature ($T_{t2R} = T_{t3R}$) can be developed by noting that

$$T_3 = T_{t3} - \frac{V_3^2}{2g_c c_p} = T_{t3R} - \frac{V_{3R}^2}{2g_c c_p}$$

Then

$$T_{t3R} = T_{t3} + \frac{V_{3R}^2 - V_3^2}{2g_c c_p}$$

or

$$T_{i3R} = T_{i3} + \frac{V_3^2}{2g_c c_p} \left[\cos^2 \alpha_3 + \left(\sin \alpha_3 + \frac{\omega r}{V_3} \right)^2 - 1 \right] \quad (9.113)$$

9.5.3 Summary of Equations—Axial-Flow Turbine Stage

INPUTS:

 T_{t1} , T_{t3} , ωr , P_{t1} , M_1 , M_2 , α_1 , α_3 , c_p , γ , u_3/u_2 , and e_t or $\phi_{t\text{stator}}$ and $\phi_{t\text{rotor}}$

OUTPUTS:

 α_2 , V_2 , u_2 , v_2 , T_2 , P_{t2} , P_2 , M_{2R} , V_3 , u_3 , v_3 , T_3 , P_{t3} , P_3 , M_3 , M_{3R} , ψ , VR, oR_t , $Z_s c_x/s$, $Z_r c_x/s$, π_s , and η_s

EQUATIONS:

$$T_1 = \frac{T_{t1}}{1 + [(\gamma - 1)/2]M_1^2}$$

$$V_1 = \sqrt{\frac{2g_c c_p T_{t1}}{1 + 2/[(\gamma - 1)M_1^2]}}$$

$$u_1 = V_1 \cos \alpha_1$$

$$T_{t2} = T_{t1}$$

$$T_2 = \frac{T_{t2}}{1 + [(\gamma - 1)/2]M_2^2}$$

$$V_2 = \sqrt{\frac{2g_c c_p T_{t2}}{1 + 2/[(\gamma - 1)M_2^2]}}$$

$$\psi = \frac{g_c c_p (T_{t1} - T_{t3})}{(\omega r)^2}$$

$$\text{VR} = \frac{1}{\sqrt{2\psi}}$$

$$\alpha_2 = \sin^{-1} \frac{\psi \frac{\omega r}{V_2} - \frac{u_3}{u_2} \tan \alpha_3 \sqrt{1 + \left(\frac{u_3}{u_2} \tan \alpha_3 \right)^2} - \left(\psi \frac{\omega r}{V_2} \right)^2}{1 + \left(\frac{u_3}{u_2} \tan \alpha_3 \right)^2}$$

$$u_2 = V_2 \cos \alpha_2$$

$$v_2 = V_2 \sin \alpha_2$$

$$V_3 = \frac{u_3 \cos \alpha_2}{u_2 \cos \alpha_3} V_2$$

$$u_3 = V_3 \cos \alpha_3$$

$$v_3 = V_3 \sin \alpha_3$$

$$^oR_t = 1 - \frac{1}{2\psi} \left(\frac{V_2}{\omega r} \right)^2 \left[1 - \left(\frac{u_3 \cos \alpha_2}{u_2 \cos \alpha_3} \right)^2 \right]$$

$$T_3 = T_2 - ^oR_t (T_{t1} - T_{t3})$$

$$M_3 = M_2 \frac{V_3}{V_2} \sqrt{\frac{T_2}{T_3}}$$

$$M_{2R} = M_2 \sqrt{\cos^2 \alpha_2 + \left(\sin \alpha_2 - \frac{\omega r}{V_2} \right)^2}$$

$$M_{3R} = M_3 \sqrt{\cos^2 \alpha_3 + \left(\sin \alpha_3 + \frac{\omega r}{V_3} \right)^2}$$

$$T_{i3R} = T_{i3} + \frac{V_3^2}{2g_c c_p} \left[\cos^2 \alpha_3 + \left(\sin \alpha_3 + \frac{\omega r}{V_3} \right)^2 - 1 \right]$$

$$T_{t2R} = T_{t3R}$$

$$P_2 = P_{t1} \left(\frac{T_1}{T_{t1}} \right)^{\gamma/(\gamma-1)}$$

$$\tau_s = \frac{T_{t3}}{T_{t1}}$$

$$\frac{Z_s c_x}{s} = (2 \cos^2 \alpha_2) \left(\tan \alpha_1 + \frac{u_2}{u_1} \tan \alpha_2 \right) \left(\frac{u_1}{u_2} \right)^2$$

$$\beta_2 = \tan^{-1} \frac{v_2 - \omega r}{u_2}$$

$$\beta_3 = \tan^{-1} \frac{v_3 + \omega r}{u_3}$$

$$\frac{Z_r c_x}{s} = (2 \cos^2 \beta_3) \left(\tan \beta_2 + \frac{u_3}{u_2} \tan \beta_3 \right) \left(\frac{u_2}{u_3} \right)^2$$

I. $\phi_{t\text{stator}}$ and $\phi_{t\text{rotor}}$ given:

$$P_{t2} = \frac{P_{t1}}{1 + \phi_{t\text{stator}} [1 - (T_2/T_{t2})^{\gamma/(\gamma-1)}]}$$

$$P_2 = P_{t2} \left(\frac{T_2}{T_{t2}} \right)^{\gamma/(\gamma-1)}$$

$$P_{t2R} = P_2 \left(\frac{T_{t2R}}{T_2} \right)^{\gamma/(\gamma-1)}$$

$$P_{t3R} = \frac{P_{t2R}}{1 + \phi_{t\text{rotor}} [1 - (T_3/T_{t3R})^{\gamma/(\gamma-1)}]}$$

$$P_3 = P_{t3R} \left(\frac{T_3}{T_{t3R}} \right)^{\gamma/(\gamma-1)}$$

$$P_{t3} = P_3 \left(\frac{T_{t3}}{T_3} \right)^{\gamma/(\gamma-1)}$$

$$\pi_s = \frac{P_{t3}}{P_{t1}}$$

$$\eta_t = \frac{1 - \tau_s}{1 - \pi_s^{(\gamma-1)/\gamma}}$$

II. e_t given:

$$P_{t3} = P_{t1} \left(\frac{T_{t3}}{T_{t1}} \right)^{\gamma/[(\gamma-1)e_t]}$$

$$\pi_s = \frac{P_{t3}}{P_{t1}}$$

$$\eta_s = \frac{1 - \tau_s}{1 - \pi_s^{(\gamma-1)/\gamma}}$$

$$P_3 = P_{t3} \left(\frac{T_3}{T_{t3}} \right)^{\gamma/(\gamma-1)}$$

$$P_{t3R} = P_3 \left(\frac{T_{t3R}}{T_3} \right)^{\gamma/(\gamma-1)}$$

With polytropic efficiency specified, P_2 , P_{t2} , and P_{t2R} cannot be calculated without an additional relationship for either P_2 or P_{t2} . For estimation of P_{t2} , the program TURBN has as the user input a value of $\phi_{t\text{stator}}$.

Example 9.10

Consider mean-radius stage calculation—flow with losses.

Given:

$$T_{t1} = 1850 \text{ K}, \quad P_{t1} = 1700 \text{ kPa}, \quad M_1 = 0.4, \quad \alpha_1 = 0 \text{ deg}$$

$$T_{t3} = 1560 \text{ K}, \quad M_2 = 1.1, \quad \omega r = 450 \text{ m/s}, \quad \alpha_3 = 10 \text{ deg}$$

$$u_3/u_2 = 0.9, \quad \phi_{t\text{stator}} = 0.06, \quad \phi_{t\text{rotor}} = 0.15$$

$$\gamma = 1.3, \quad R = 0.2873 \text{ kJ/(kg} \cdot \text{K}) \quad [c_p = 1.245 \text{ kJ/(kg} \cdot \text{K})]$$

Solution:

$$T_1 = \frac{T_{t1}}{1 + [(\gamma - 1)/2]M_1^2} = \frac{1850 \text{ K}}{1 + 0.15 \times 0.4^2} = 1806.6 \text{ K}$$

$$V_1 = \sqrt{\frac{2g_c c_p T_{t1}}{1 + 2/[(\gamma - 1)M_1^2]}} = \sqrt{\frac{2 \times 1 \times 1245 \times 1850}{1 + 2/(0.3 \times 0.4^2)}} = 328.6 \text{ m/s}$$

$$u_1 = V_1 \cos \alpha_1 = 328.6 \text{ m/s}$$

$$v_1 = V_1 \sin \alpha_1 = 0$$

$$T_{t2} = T_{t1} = 1850 \text{ K}$$

$$T_2 = \frac{T_{t2}}{1 + [(\gamma - 1)/2]M_2^2} = \frac{1850 \text{ K}}{1 + 0.15 \times 1.1^2} = 1565.8 \text{ K}$$

$$V_2 = \sqrt{\frac{2g_c c_p T_{t2}}{1 + 2/[(\gamma - 1)M_2^2]}} = \sqrt{\frac{2 \times 1 \times 1245 \times 18}{1 + 2/(0.3 \times 1.1^2)}} = 841.2 \text{ m/s}$$

$$\psi = \frac{g_c c_p (T_{t1} - T_{t3})}{(\omega r)^2} = \frac{1245(1850 - 1560)}{450^2} = 1.78296$$

$$\text{VR} = \frac{1}{\sqrt{2}\psi} = \frac{1}{\sqrt{2 \times 1.78296}} = 0.5296$$

$$\alpha_2 = \sin^{-1} \frac{\left(\psi \frac{\omega r}{V_2} \right) - \left(\frac{u_3}{u_2} \tan \alpha_3 \right) \sqrt{1 + \left(\frac{u_3}{u_2} \tan \alpha_3 \right)^2 - \left(\psi \frac{\omega r}{V_2} \right)^2}}{1 + \left(\frac{u_3}{u_2} \tan \alpha_3 \right)^2}$$

$$\psi \frac{\omega r}{V_2} = 1.78296 \left(\frac{450}{841.2} \right) = 0.95379$$

$$\frac{u_3}{u_2} \tan \alpha_3 = 0.9 \tan 10 \text{ deg} = 0.15869$$

$$\alpha_2 = \sin^{-1} \frac{0.95379 - 0.15869 \sqrt{1 + 0.15869^2 - 0.95379^2}}{1.015869^2}$$

$$= \sin^{-1} 0.87776 = 61.37 \text{ deg}$$

$$u_2 = V_2 \cos \alpha_2 = 841.2 \cos 61.37 \text{ deg} = 403.1 \text{ m/s}$$

$$v_2 = V_2 \sin \alpha_2 = 841.2 \sin 61.37 \text{ deg} = 738.3 \text{ m/s}$$

$$\Phi = \frac{u_2}{\omega r} = \frac{403.1}{450} = 0.8958$$

$$V_3 = \frac{u_3 \cos \alpha_2}{u_2 \cos \alpha_3} V_2 = 0.9 \left(\frac{\cos 61.37 \text{ deg}}{\cos 10 \text{ deg}} \right) (841.2) = 368.4 \text{ m/s}$$

$$u_3 = V_3 \cos \alpha_3 = 368.4 \cos 10 \text{ deg} = 362.8 \text{ m/s}$$

$$v_3 = V_3 \sin \alpha_3 = 368.4 \sin 10 \text{ deg} = 64.0 \text{ m/s}$$

$$\begin{aligned} {}^oR_t &= 1 - \frac{1}{2\psi} \left(\frac{V_2}{\omega r} \right)^2 \left[1 - \left(\frac{u_3 \cos \alpha_2}{u_2 \cos \alpha_3} \right)^2 \right] \\ &= 1 - \frac{1}{2 \times 1.78296} \left(\frac{841.2}{450} \right)^2 \left[1 - \left(0.9 \frac{\cos 61.37 \text{ deg}}{\cos 10 \text{ deg}} \right)^2 \right] = 0.2080 \end{aligned}$$

$$T_3 = T_2 - {}^oR_t(T_{t1} - T_{t3}) = 1565.8 - 0.2080(1850 - 1560) = 1505.5 \text{ K}$$

$$M_3 = M_2 \frac{V_3}{V_2} \sqrt{\frac{T_2}{T_3}} = 1.1 \left(\frac{368.4}{841.2} \right) \sqrt{\frac{1565.8}{1505.5}} = 0.4913$$

$$\begin{aligned} M_{2R} &= M_2 \sqrt{\cos^2 \alpha_2 + \left(\sin \alpha_2 - \frac{\omega r}{V_2} \right)^2} \\ &= 1.1 \sqrt{\cos^2 61.37 \text{ deg} + \left(\sin 61.37 \text{ deg} - \frac{450}{841.2} \right)^2} = 0.6481 \end{aligned}$$

$$\begin{aligned} M_{3R} &= M_3 \sqrt{\cos^2 \alpha_3 + \left(\sin \alpha_3 + \frac{\omega r}{V_3} \right)^2} \\ &= 0.4913 \sqrt{\cos^2 10 \text{ deg} + \left(\sin 10 \text{ deg} + \frac{450}{368.4} \right)^2} = 0.8390 \end{aligned}$$

$$\begin{aligned} T_{t3R} &= T_{t3} + \frac{V_3^2}{2g_c c_p} \left[\cos^2 \alpha_3 + \left(\sin \alpha_3 + \frac{\omega r}{V_3} \right)^2 - 1 \right] \\ &= 1560 + \frac{368.4^2}{2 \times 1 \times 1245} \left[\cos^2 10 \text{ deg} + \left(\sin 10 \text{ deg} + \frac{450}{368.4} \right)^2 - 1 \right] \\ &= 1664.4 \text{ K} \end{aligned}$$

$$T_{t2R} = T_{t3R} = 1664.4 \text{ K}$$

$$\tau_s = \frac{T_{t3}}{T_{t1}} = \frac{1560}{1850} = 0.8432$$

$$\frac{Z_s c_x}{s} = (2 \cos^2 \alpha_2) \left(\tan \alpha_1 + \frac{u_2}{u_1} \tan \alpha_2 \right) \left(\frac{u_1}{u_2} \right)^2$$

$$\begin{aligned} &= (2 \cos^2 61.37 \text{ deg}) \left(\tan 0 \text{ deg} + \frac{403.1}{328.6} \tan 61.37 \text{ deg} \right) \left(\frac{328.6}{403.1} \right)^2 \\ &= 0.6857 \end{aligned}$$

$$\beta_2 = \tan^{-1} \frac{v_2 - \omega r}{u_2} = \tan^{-1} \frac{738.3 - 450}{403.1} = 35.57 \text{ deg}$$

$$\beta_3 = \tan^{-1} \frac{v_3 + \omega r}{u_3} = \tan^{-1} \frac{64.0 + 450}{362.8} = 54.78 \text{ deg}$$

$$\begin{aligned} \frac{Z_r c_x}{s} &= (2 \cos^2 \beta_3) \left(\tan \beta_2 + \frac{u_3}{u_2} \tan \beta_3 \right) \left(\frac{u_2}{u_3} \right)^2 \\ &= (2 \cos^2 54.78 \text{ deg})(\tan 35.573 \text{ deg} + 0.9 \tan 54.78 \text{ deg}) \left(\frac{1}{0.9} \right)^2 \\ &= 1.6330 \end{aligned}$$

$$P_1 = P_{t1} \left(\frac{T_1}{T_{t1}} \right)^{\gamma/(\gamma-1)} = 1700 \left(\frac{1806.6}{1850} \right)^{1.3/0.3} = 1533.8 \text{ kPa}$$

$$\begin{aligned} P_{t2} &= \frac{P_{t1}}{1 + \phi_{t \text{ stator}} [1 - (T_2/T_{t2})^{\gamma/(\gamma-1)}]} \\ &= \frac{1700}{1 + 0.06 [1 - (1565.8/1850)^{1.3/0.3}]} = 1649.1 \text{ kPa} \end{aligned}$$

$$P_2 = P_{t2} \left(\frac{T_2}{T_{t2}} \right)^{\gamma/(\gamma-1)} = 1649.1 \left(\frac{1565.8}{1850} \right)^{1.3/0.3} = 800.5 \text{ kPa}$$

$$P_{t2R} = P_2 \left(\frac{T_{t2R}}{T_2} \right)^{\gamma/(\gamma-1)} = 800.5 \left(\frac{1664.4}{1565.8} \right)^{1.3/0.3} = 1043.0 \text{ kPa}$$

$$\begin{aligned} P_{t3R} &= \frac{P_{t2R}}{1 + \phi_{t \text{ rotor}} [1 - (T_3/T_{t3R})^{\gamma/(\gamma-1)}]} \\ &= \frac{1043.0}{1 + 0.15 [1 - (1505.5/1664.4)^{1.3/0.3}]} = 990.6 \text{ kPa} \end{aligned}$$

$$P_3 = P_{t3R} \left(\frac{T_3}{T_{t3R}} \right)^{\gamma/(\gamma-1)} = 990.6 \left(\frac{1505.5}{1664.4} \right)^{1.3/0.3} = 641.3 \text{ kPa}$$

$$P_{t3} = P_3 \left(\frac{T_{t3}}{T_3} \right)^{\gamma/(\gamma-1)} = 641.3 \left(\frac{1560}{1505.5} \right)^{1.3/0.3} = 748.1 \text{ kPa}$$

$$\pi_s = \frac{P_{t3}}{P_{t1}} = \frac{748.1}{1700} = 0.441$$

$$\eta_s = \frac{1 - \tau_s}{1 - \pi_s^{(\gamma-1)/\gamma}} = \frac{1 - 0.8432}{1 - 0.4401^{0.3/1.3}} = 90.87\%$$

9.5.4 Flow Path Dimensions

9.5.4.1 Annulus area. The annulus area (see Fig. 9.26) at any station of a turbine stage is based on the flow properties (T_t , P_t , Mach number, and flow angle) at the mean radius and the total mass flow rate. Equation (9.8) is the easiest equation to use to calculate the flow area at any station i :

$$A_i = \frac{\dot{m}\sqrt{T_{ti}}}{P_{ti}(\cos \alpha_i)\text{MFP}(M_i)}$$

By using the relationships of Fig. 9.26, the radii at any station i can be determined, given the flow annulus area [Eq. (9.8)] and either the mean radius r_m or the hub/tip ratio r_h/r_t .

9.5.4.2 Axial dimensions and number of blades. Figure 9.69 shows the cross section of a typical turbine stage that can be used to estimate its axial length. The chord/height ratio c/h of turbine blades varies from about 0.3 to 1.0. Assuming constant chord length and circular arc chamber line, the program TURBN calculates the axial blade widths W_s and W_r of a stage, the blade spacings $W_s/4$ and $W_r/4$, and the number of blades based on user inputs of the tangential force coefficient Z and chord/height ratio c/h for both the stator and rotor blades. A minimum width of $\frac{1}{4}$ in. (0.6 cm) and spacing of $\frac{1}{8}$ in. (0.3 cm) are used in the plot of a turbine cross section and calculation of axial length.

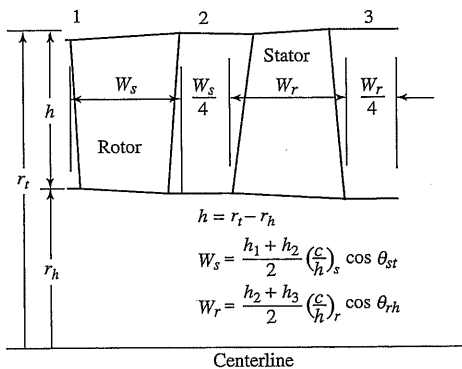


Fig. 9.69 Typical axial dimensions of a turbine stage.

The stagger angle θ of a blade depends on the shape of the chamber line and blade angles γ_i and γ_e (see Fig. 9.62). For a circular arc chamber line, the stagger angle θ is simply given by $\theta = (\gamma_e - \gamma_i)/2$. For constant-chord blades, the axial chord (and axial blade width) is greatest where the stagger angle is closest to zero. This normally occurs at the tip of the stator and hub of the rotor blades. For estimation purposes, a turbine blade's incidence angle is normally small and can be considered to be zero. Thus $\gamma_i = \alpha_i$. The blade's exit angle γ_e can be obtained using Eq. (9.89) for the exit deviation. However, Eq. (9.89) requires that the solidity ($\sigma = c/s$) be known. For known flow conditions (α_1 , α_2 , u_2/u_1 , α_2 , α_3 , and u_3/u_2) and given tangential force coefficients (Z_s and Z_r), Eqs. (9.98a) and (9.98b) will give the required axial chord/spacing ratio c_x/s for the stator and rotor, respectively. An initial guess for the blade's solidity σ is needed to obtain the stagger angle θ from c_x/s .

After the solidities are determined at the hub, mean, and tip that give the desired tangential force coefficient Z , the number of required blades follows directly from the chord/height ratio c/h , the circumference, and the blade spacing at each radius. The following example shows the calculations needed to find the axial blade width and number of blades.

Example 9.11

Here we consider the turbine stator of Example 9.10 with a mass flow rate of 60 kg/s, a mean radius of 0.3 m, a tangential force coefficient Z_s of 0.9, and a chord/height ratio c/h of 1.0. The flow annulus areas and radii at stations 1 and 2 are as follows.

Station 1:

$$\text{MFP}(M_1) = 0.024569$$

$$A_1 = \frac{\dot{m}\sqrt{T_{t1}}}{P_{t1}\text{MFP}(M_1)(\cos \alpha_1)} = \frac{60\sqrt{1850}}{1,700,00 \times 0.024569 \times 1} \\ = 0.0617788 \text{ m}^2$$

$$h_1 = \frac{A_1}{2\pi r_m} = \frac{0.0617788}{0.6\pi} = 0.03278 \text{ m}$$

$$r_{t1} = 0.3164 \text{ m} \quad r_{h1} = 0.2836 \text{ m}$$

$$v_{1h} = v_{1m} = v_{1t} = 0$$

Station 2:

$$\text{MFP}(M_2) = 0.039042$$

$$A_2 = \frac{\dot{m}\sqrt{T_{t2}}}{P_{t2}\text{MFP}(M_2)(\cos \alpha_2)} \\ = \frac{60\sqrt{1850}}{1,649,100 \times 0.039042 \times \cos 61.37 \text{ deg}} = 0.083654 \text{ m}^2$$

$$h_2 = \frac{A_2}{2\pi r_m} = \frac{0.083654}{0.6\pi} = 0.04438 \text{ m}$$

$$r_{t2} = 0.3222 \text{ m} \quad r_{h2} = 0.2778 \text{ m}$$

$$v_{2h} = v_{2m} \frac{r_m}{r_{2h}} = 738.3 \left(\frac{0.3}{0.2778} \right) = 797.3 \text{ m/s}$$

$$\alpha_{2h} = \tan^{-1} \frac{v_{2h}}{u_2} = \tan^{-1} \frac{797.3}{403.1} = 63.18 \text{ deg}$$

$$v_{2t} = v_{2m} \frac{r_m}{r_{2t}} = 738.3 \left(\frac{0.3}{0.3222} \right) = 687.4 \text{ m/s}$$

$$\alpha_{2t} = \tan^{-1} \frac{v_{2t}}{u_2} = \tan^{-1} \frac{687.4}{403.1} = 59.61 \text{ deg}$$

The chord of the stator is

$$c = \frac{c h_1 + h_2}{h} = 1.0 \frac{0.03278 + 0.04438}{2} = 0.03858 \text{ m}$$

For the specified tangential force coefficient Z_s , we calculate the stagger angle, solidity, and spacing of the stator at the mean line, hub, and tip.

Mean line:

$$\begin{aligned} Z_s \left(\frac{c_x}{s} \right)_m &= (2 \cos^2 \alpha_{2m}) \left(\tan \alpha_{1m} + \frac{u_2}{u_1} \tan \alpha_{2m} \right) \left(\frac{u_1}{u_2} \right)^2 \\ &= (2 \cos^2 61.37 \text{ deg}) \left(\tan 0 \text{ deg} + \frac{403.1}{328.6} \tan 61.37 \text{ deg} \right) \\ &\times \left(\frac{328.6}{403.1} \right)^2 = 0.6857 \end{aligned}$$

$$\left(\frac{c_x}{s} \right)_m = \frac{0.6857}{0.9} = 0.7619$$

$$\gamma_{1m} = \alpha_{1m} = 0$$

Initially, we assume a solidity σ of 1.0. Then,

$$\gamma_{2m} = \frac{\gamma_{1m} + 8\sqrt{\sigma_m} \alpha_{2m}}{8\sqrt{\sigma_m} - 1} = \frac{0 + 8\sqrt{1} \cdot 61.37}{8\sqrt{1} - 1} = 70.14 \text{ deg}$$

$$\theta_m = \frac{\gamma_{2m} - \gamma_{1m}}{2} = \frac{70.14}{2} = 35.07 \text{ deg}$$

$$\sigma_m = \frac{(c_x/s)_m}{\cos \theta_m} = \frac{0.7619}{\cos 35.07 \text{ deg}} = 0.9309$$

After several iterations, the results are $\gamma_{2m} = 70.49$ deg, $\theta_m = 35.25$ deg, and $\sigma_m = 0.9329$. The blade spacing s is 0.04135 m, and the axial chord is 0.03150 m.

Hub:

$$\begin{aligned} Z_s \left(\frac{c_x}{s} \right)_h &= (2 \cos^2 \alpha_{2h}) \left(\tan \alpha_{1h} + \frac{u_2}{u_1} \tan \alpha_{2h} \right) \left(\frac{u_1}{u_2} \right)^2 \\ &= (2 \cos^2 63.18 \text{ deg}) \left(\tan 0 \text{ deg} + \frac{403.1}{328.6} \tan 63.18 \text{ deg} \right) \\ &\times \left(\frac{328.6}{403.1} \right)^2 = 0.6565 \\ \left(\frac{c_x}{s} \right)_h &= \frac{0.6565}{0.9} = 0.7294 \end{aligned}$$

$$\gamma_{1h} = \alpha_{1h} = 0$$

Initially, we assume a solidity σ of 1.0. Then,

$$\begin{aligned} \gamma_{2h} &= \frac{\gamma_{1h} + 8\sqrt{\sigma_h} \alpha_{2h}}{8\sqrt{\sigma_h} - 1} = \frac{0 + 8\sqrt{1} \cdot 63.18}{8\sqrt{1} - 1} = 72.21 \text{ deg} \\ \theta_h &= \frac{\gamma_{2h} - \gamma_{1h}}{2} = \frac{72.21}{2} = 36.10 \text{ deg} \\ \sigma_h &= \frac{(c_x/s)_h}{\cos \theta_h} = \frac{0.7294}{\cos 36.10 \text{ deg}} = 0.9027 \end{aligned}$$

After several iterations, the results are $\gamma_{2h} = 72.73$ deg, $\theta_h = 36.37$ deg, and $\sigma_h = 0.9058$. The blade spacing s is 0.04259 m, and the axial chord is 0.03107 m.

Tip:

$$\begin{aligned} Z_s \left(\frac{c_x}{s} \right)_t &= (2 \cos^2 \alpha_{2t}) \left(\tan \alpha_{1t} + \frac{u_2}{u_1} \tan \alpha_{2t} \right) \left(\frac{u_1}{u_2} \right)^2 \\ &= (2 \cos^2 59.61 \text{ deg}) \left(\tan 0 \text{ deg} + \frac{403.1}{328.6} \tan 59.61 \text{ deg} \right) \\ &\times \left(\frac{328.6}{403.1} \right)^2 = 0.7115 \\ \left(\frac{c_x}{s} \right)_t &= \frac{0.7115}{0.9} = 0.7905 \\ \gamma_{1t} &= \alpha_{1t} = 0 \end{aligned}$$

Table 9.13 Summary of Example 9.11 results

Location	Average radius, m	Solidity	Spacing, m	Number of blades	Axial chord, m
Tip	0.3193	0.9555	0.04038	49.7	0.03192
Mean	0.3000	0.9329	0.04135	45.6	0.03150
Hub	0.2807	0.9058	0.04259	41.4	0.03107

Initially, we assume a solidity σ of 1.0:

$$\gamma_{2t} = \frac{\gamma_{1t} + 8\sqrt{\sigma_t}\alpha_{2t}}{8\sqrt{\sigma_t} - 1} = \frac{0 + 8\sqrt{1}59.61}{8\sqrt{1} - 1} = 68.13 \text{ deg}$$

$$\theta_t = \frac{\gamma_{2t} - \gamma_{1t}}{2} = \frac{68.13}{2} = 34.06 \text{ deg}$$

$$\sigma_t = \frac{(c_x/s)_t}{\cos \theta_t} = \frac{0.7905}{\cos 34.06 \text{ deg}} = 0.9542$$

After several iterations, the results are $\gamma_{2t} = 68.35$ deg, $\theta_t = 34.18$ deg, and $\sigma_t = 0.9555$. The blade spacing s is 0.04038 m, and the axial chord is 0.03192 m.

For this stator blade with a chord of 0.03858 m, we require the information in Table 9.13. Thus the number of required stator blades is 50, which will have a mean-radius spacing s of 0.03770 m and solidity σ of 1.023 (= 0.03858/0.03770) on the mean radius. The blade has an axial width W_s of 0.03192 m (see Fig. 9.69).

9.5.4.3 Blade profile. The shapes of turbine stator and rotor blades are based on airfoil shapes developed specifically for turbine applications. Two airfoil shapes are included in the program TURBN to sketch the blade shapes for a stage: the C4 and T6 British profiles. The base profile of the C4 airfoil is listed in Table 9.14 and shown in Fig. 9.70 for a 10% thickness. Table 9.15 and Fig. 9.71 give the base profile of the T6 airfoil for a 10% thickness. The program TURBN assumes a circular arc mean line for sketching the blade shapes.

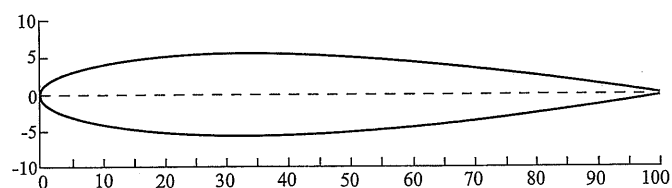


Fig. 9.70 The C4 turbine airfoil base profile.

Table 9.14 C4 airfoil profile ($t/c = 0.10$)^{a,b}

x/c, %	y/c, %	x/c, %	y/c, %
0.0	0.0	40	4.89
1.25	1.65	50	4.57
2.5	2.27	60	4.05
5	3.08	70	3.37
7.5	3.62	80	2.54
10	4.02	90	1.60
15	4.55	95	1.06
20	4.83	100	0.0
30	5.00		

^aLeading-edge radius = 0.12 t .

^bTrailing-edge radius = 0.06 t .

Table 9.15 T6 airfoil profile ($t/c = 0.10$)^{a,b}

x/c, %	y/c, %	x/c, %	y/c, %
0.0	0.0	40	5.00
1.25	1.17	50	4.67
2.5	1.54	60	3.70
5	1.99	70	2.51
7.5	2.37	80	1.42
10	2.74	90	0.85
15	3.4	95	0.72
20	3.95	100	0.0
30	4.72		

^aLeading-edge radius = 0.12 t .

^bTrailing-edge radius = 0.06 t .

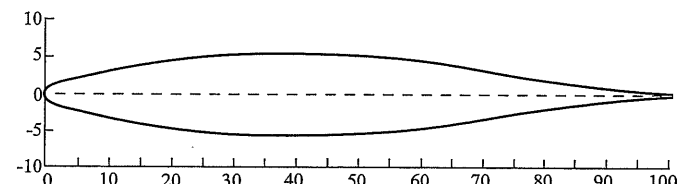


Fig. 9.71 The T6 turbine airfoil base profile.

Example 9.12

Consider a single-stage turbine using the computer program TURBN.

Given:

$$\dot{m} = 200 \text{ lbm/s}, \quad M_1 = 0.4, \quad T_{t1} = 3400^\circ\text{R}$$

$$T_{t3} = 2860^{\circ}\text{R}, \quad M_2 = 1.1, \quad \omega r = 1500 \text{ ft/s}, \quad r_m = 12 \text{ in.}$$

$$P_{t1} = 250 \text{ psia}, \quad \alpha_1 = 0 \text{ deg}, \quad \alpha_3 = 0 \text{ deg}, \quad \gamma = 1.3$$

$$R = 53.40 \text{ ft} \cdot \text{lbf}/(\text{lbfm} \cdot {}^\circ\text{R}), \quad u_3/u_2 = 0.90, \quad \psi_{t \text{ stator}} = 0.06, \quad \phi_{t \text{ rotor}} = 0.15$$

Solution: The program TURBN is run with α_2 as the unknown. The results are given in Table 9.16 with the hub and tip tangential velocities based on free-vortex swirl distribution. The cross section of the stage sketched by the computer program is shown in Fig. 9.72 for stator $c/h = 0.8$ and rotor $c/h = 0.6$. The very high AN^2 of $4.18 \times 10^{10} \text{ in.}^2 \cdot \text{rpm}^2$ at a relative total temperature of 3052°R is not possible with current materials unless the blades are cooled. Also, the high rim speed of about 1206 ft/s would require existing materials to be cooled.

9.5.5 Axial-Flow Turbine Stage— α_2 Known

The preceding method of calculation assumed that α_2 was unknown. The program TURBN will handle the case when any one of the following four variables is unknown:

α_2 , T_{t3} , α_3 , or M_2

When T_{t3} is unknown, Eqs. (9.20) and (9.103) are solved for T_{t3} , giving

$$T_{t3} = T_{t1} - \frac{\omega r V_2}{g c_p c_p} \left(\sin \alpha_2 + \frac{u_3}{u_2} \cos \alpha_2 \tan \alpha_3 \right) \quad (9.114)$$

When α_3 is unknown, Eqs. (9.20) and (9.103) are solved for α_3 , giving

$$\tan \alpha_3 = \frac{1}{u_3/u_2} \left(\frac{\psi}{\cos \alpha_2} \frac{\omega \gamma}{V_2} - \tan \alpha_2 \right) \quad (9.115)$$

When M_2 is unknown, the velocity at station 2 (v_2) is obtained from Eq (9.103), giving

$$V_2 = \frac{\psi \omega r}{\sin \alpha_2 + (u_3/u_2) \cos \alpha_2 \tan \alpha_3} \quad (9.116)$$

Then M_2 is obtained from Eq. (9.104) rewritten as

$$M_2 = \frac{V_2}{\sqrt{(\gamma - 1)g_c c_p T_{r2} - [(\gamma - 1)/2] V_2^2}} \quad (9.117)$$

9.5.6 Axial-Flow Turbine Stage Analysis—No Exit Swirl

Consider the flow through a single-stage turbine as shown in Fig. 9.73 with zero exit swirl. We will consider the case where there is no exit swirl ($v_3 = 0$).

Table 9.16 Results for Example 9.12 axial-flow turbine stage calculation using TURBINE

Property	1h	Station							
		1m	1t	2h	2m	2t	2Rm	3h	3m
R_i	3400	3400	3400	3400	3400	3400	3052	2860	2860
R_i'	3320	3320	2767	2878	2957	2878	2768	2768	2769
P_i	250.0	250.0	242.5	242.5	242.5	242.5	144.4	109.0	109.0
P_i'	225.6	225.6	99.2	117.7	132.4	117.7	94.6	94.6	94.7
M	0.400	0.400	1.236	1.100	1.100	1.100	0.827	0.474	0.474
V	ft/s	1089	1089	3071	2789	2569	1611	2057	1178
t	ft/s	1089	1089	1282	1282	1282	1282	1153	1153
τ_s	deg	0	0	2791	2477	2226	977	1703	239
R_i	deg	0	0	65.34	62.64	60.07	—	11.68	10.00
Radius	in.	11.04	12.00	12.96	10.65	12.00	13.35	12.00	10.20
Hub:	$A_1 = 144.31 \text{ in.}^2$								
Mean:	$A_2 = 203.72 \text{ in.}^2$								
Tip:	$A_3 = 271.04 \text{ in.}^2$								
η_s :	$\tau_s = 0.8412$	$\pi_s = 0.4359$	$\text{RPM} = 14,324$						$\phi = 0.8544$
η_s :	$\tau_s = 0.9108\%$	$\text{RPM}^2 \text{ at } 2 = 4.18 \times 10^{10} \text{ in.}^2 \cdot \text{rpm}^2$						$\psi = 1.7868$	

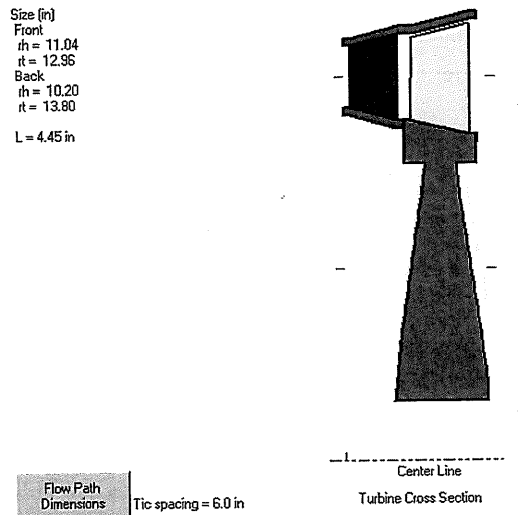


Fig. 9.72 Sketch of cross section for turbine stage of Example 9.12 from TURBN.

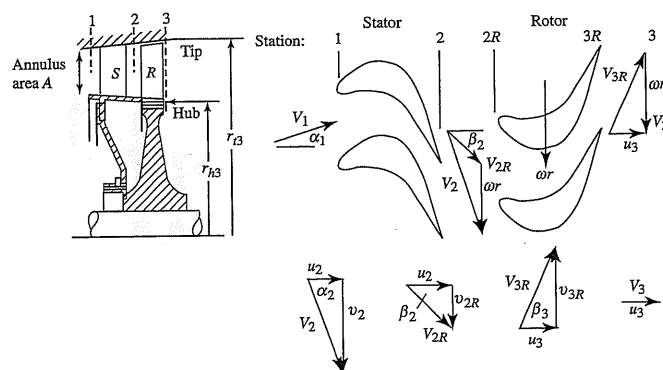


Fig. 9.73 Generalized turbine stage, zero exit swirl.

$\alpha_3 = 0$) and the axial velocities at stations 2 to 3 are the same ($u_2 = u_3$). The flows through the nozzle (stator) and rotor are assumed to be adiabatic. For solution, we assume the following data are known:

$$M_2, T_{t1}, T_{t3}, \omega r, c_p, \text{ and } \gamma$$

The equations for solution of a zero exit swirl, axial-flow turbine based on these known data are developed in this section.

At station 2, v_2 is given by

$$\begin{aligned} V_2 &= \sqrt{\frac{2g_c c_p T_{t2}}{1 + 2/[(\gamma - 1)M_2^2]}} \\ &= \omega r \sqrt{\frac{2\psi/(1 - \tau_s)}{1 + 2/[(\gamma - 1)M_2^2]}} \end{aligned} \quad (9.118)$$

and α_2 by

$$\sin \alpha_2 = \psi \frac{\omega \gamma}{V_2} = \sqrt{(1 - \tau_s) \frac{\psi}{2} \left[1 + \frac{2}{(\gamma - 1)M_2^2} \right]} \quad (9.119)$$

Because the axial velocities at stations 2 and 3 are equal, the velocity at station 3 is given by

$$V_3 = V_2 \cos \alpha_2 \quad (9.120)$$

The degree of reaction is given by Eq. (9.87):

$$R_t = 1 - \frac{\psi}{2}$$

The stage exit Mach number M_3 is derived as follows. Given that

$$\frac{M_3}{M_2} = \frac{u_3/a_3}{V_2/a_2} = \frac{u_2 a_2}{V_2 a_3} = \cos \alpha_2 \sqrt{\frac{T_2}{T_3}}$$

Then from Eq. (9.81b), we write

$$R_t = \frac{T_2 - T_3}{T_{t1} - T_{t3}} = 1 - \frac{\psi}{2}$$

which allows the temperature ratio T_2/T_3 to be written as

$$\frac{T_2}{T_3} = \frac{1}{1 - (T_{t2}/T_2)(1 - \tau_s)(1 - \psi/2)} \quad (9.121)$$

Thus the Mach number M_3 can be written as

$$M_3 = \frac{M_2 \cos \alpha_2}{\sqrt{1 - (1 - \tau_s)(1 - \psi/2)\{1 + (\gamma - 1)/2\}M_2^2}} \quad (9.122)$$

A compact equation for the rotor exit relative Mach number M_{3R} is developed as follows. Since

$$\frac{M_{3R}}{M_2} = \frac{V_{3R}}{a_3} \frac{a_2}{V_2} = \frac{V_{3R}}{V_2} \sqrt{\frac{T_2}{T_3}}$$

the velocity ratio is obtained by first writing

$$V_{3R}^2 = u^2 + (\omega r)^2 = V_2^2 - v_2^2 + (\omega r)^2$$

Thus

$$\begin{aligned} \frac{V_{3R}^2}{V_2^2} &= 1 - \frac{v_2^2}{V_2^2} + \frac{(\omega r)^2}{V_2^2} = 1 - \left(\frac{\omega r}{V_2} \right)^2 \left[\left(\frac{v_2}{\omega r} \right)^2 - 1 \right] \\ &= 1 - \left(\frac{\omega r}{V_2} \right)^2 (\psi^2 - 1) \end{aligned}$$

Since

$$\frac{M_{3R}}{M_2} = \frac{V_{3R}}{V_2} \sqrt{\frac{T_2}{T_3}}$$

then by using Eq. (9.121), the Mach number ratio is found by

$$\frac{M_{3R}}{M_2} = \sqrt{\frac{1 - (\omega r/V_2)^2(\psi^2 - 1)}{1 - (T_{t2}/T_2)(1 - \tau_s)(1 - \psi/2)}} \quad (9.123)$$

which with Eq. (9.119) becomes (and is actually used as)

$$\frac{M_{3R}}{M_2} = \sqrt{\frac{1 - (1 - \tau_s) \frac{\psi^2 - 1}{2\psi} \left[1 + \frac{2}{(\gamma - 1)M_2^2} \right]}{1 - (1 - \tau_s) \left(1 - \frac{\psi}{2} \right) \left(1 + \frac{\gamma - 1}{2} M_2^2 \right)}} \quad (9.124)$$

This equation contains an interesting and unexpected piece of guidance for the design of turbine stages. To ensure that stator cascade choking controls the turbine mass flow rate, M_2 should be greater than unity and M_{3R} should be less than unity. Equation (9.124) reveals, however, that when the stage loading coefficient is unity (degree of reaction is 0.5), the opposite must be true. Therefore, even though it would appear preferable to aim for a degree of reaction near 0.5 to balance the difficulty of designing the stator and rotor airfoils, the requirement to reduce M_{3R} translates to lower allowable values of the degree of reaction and correspondingly higher stage loadings. In actual practice, the degree of reaction is usually found in the range of 0.2 to 0.4, so that a substantial, but minority, fraction of the overall static enthalpy (and static pressure) drop still takes place across the rotor and is available to prevent the separation of the suction surface boundary layer. It is important to bear in mind that even turbine airfoil boundary layers can separate, and when they do, the effect on efficiency (and heat transfer) is usually disastrous.

The rotor relative total temperature ($T_{t2R} = T_{t3R}$), which is useful for heat transfer and structural analyses, is given by Eq. (9.113). For our case of zero exit swirl and constant axial velocity ($u_3 = u_2$), this equation reduces to

$$\frac{T_{t3R}}{T_{t2}} = \tau_s + \frac{1 - \tau_s}{2\psi} \quad (9.125)$$

Example 9.13

To illustrate the application of this method, a single-stage turbine with zero exit swirl will be designed for the following conditions:

$$\begin{array}{ll} M_1 = 0.4 & M_2 = 1.10 \\ \omega r = U = 300 \text{ m/s} & T_{t2} = T_{t1} = 1400 \text{ K} \\ R = 0.2872 \text{ kJ/(kg} \cdot \text{K}) & g_c c_p = 1.158 \text{ kJ/(kg} \cdot \text{K}) \\ T_{t3} = 1260 \text{ K} & \gamma = 1.33 \\ \frac{T_{t3}}{T_{t1}} = 0.900 & \psi = 1.8006 \text{ Eq. (9.20)} \end{array}$$

If one chooses to assume $e_t = 0.90$, the results are

$$\begin{array}{ll} {}^\circ R_t = 0.0997 & M_{3R} = 0.8756 \quad \text{Eq. (9.124)} \\ \alpha_2 = 47.35 \text{ deg} & T_{t3R} = 1299 \text{ K} \quad \text{Eq. (9.125)} \\ M_3 = 0.7498 & \Phi = 1.6586 \quad \text{Eq. (9.78a)} \\ \pi_s = 0.6239 & \eta_t = 0.9053 \quad \text{Eq. (9.76)} \end{array}$$

These results provide the basis for step-by-step calculations leading to the summary of flow properties given in Table 9.17.

Table 9.17 Results for Example 9.13 axial-flow turbine state calculation with zero exit swirl

Property	Station				
	1	2	2R	3R	3
T_t	1400.0	1400.0	1298.9	1298.9	1260.0
T	1364.0	1167.0	1167.0	2012.7	2012.7
P_t	1.0000	?	?	0.7053	0.6239
$\frac{P}{P_{t1}}$	0.9003	?	?	0.4364	0.4364
M	0.400	1.100	0.8586	0.8756	0.7498
V m/s	288.7	734.4	552.5	581.0	497.6
u m/s	288.7	497.6	497.6	497.6	497.6
v m/s	0	540.2	240.2	300.0	0
α deg	0	47.35	—	—	0
β deg	—	—	25.76	31.09	—

9.5.6.1 General solution. When γ and e_t are fixed, closer examination of the turbine stage design equation set reveals that the results depend only on the dimensionless quantities M_2 , τ_s , and ψ . Under these conditions, it is therefore possible to generate graphical representations that reveal the general tendencies of such turbine stages and serve the important purpose of defining the limits of reasonable stage designs.

This has been done for typical ranges of the prevailing dimensionless parameters and γ values of 1.33 and 1.3; the results are presented in Figs. 9.74 and 9.75, respectively. These charts may be used to obtain initial ballpark-stage design estimates and also reveal some important trends. If values of M_{3R} less than 1 and stage loading coefficients ψ less than or equal to 2.0 are taken as reasonable limits, it is clear that better (i.e., lower) values of ψ are available for the same ΔT_t as τ_s decreases (lower inlet temperatures) and/or ωr increases (higher wheel speeds). By noting that ψ does not depend on M_2 [Eq. (9.87)], it is also clear that M_2 determines only M_{3R} . Larger values of M_2 are desirable because they reduce the annulus flow area A and the rotating airfoil centrifugal stresses, and ensure choking of the stator airfoil passages over a wider turbine operating range; but Figs. 9.74 and 9.75 show that increasing M_2 reduces the number of acceptable solutions. Finally, all other things being equal, stages having lower τ_s (i.e., more energy extraction) suffer the dual disadvantages of increased stage loading coefficient ψ and increased annulus flow area A .

Figures 9.74 and 9.75 exhibit an extremely interesting mathematical behavior in the region where all the curves for a value of M_2 appear to, and indeed do, pass through a single point. This fact may be verified by equating the numerator and denominator on the right side of the equals sign in Eq. (9.124), and this reveals that $M_{3R} = M_2$ is independent of either M_2 or τ_s provided only that

$$\psi^2 - 1 = \frac{\gamma - 1}{2} (2\psi - \psi^2) M_2^2$$

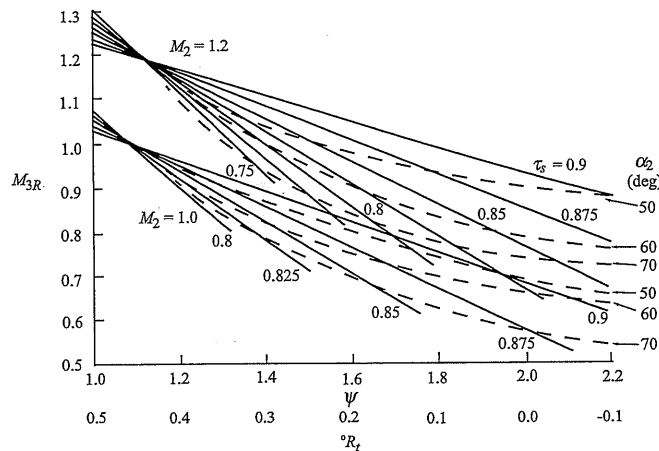


Fig. 9.74 Generalized turbine stage behavior, zero exit swirl ($\gamma = 1.33$).

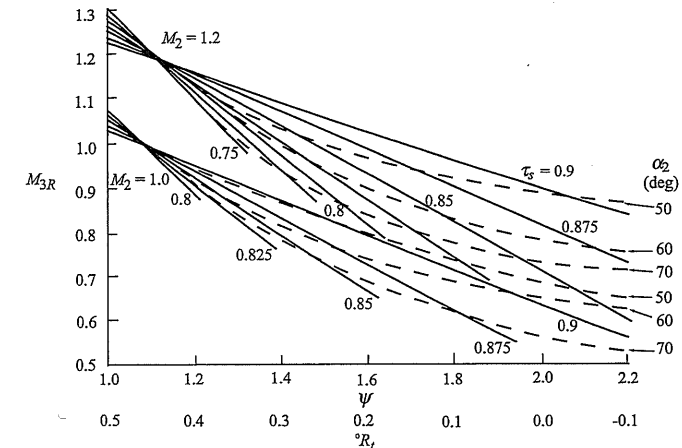


Fig. 9.75 Generalized turbine stage behavior, zero exit swirl ($\gamma = 1.3$).

Hence, for each γ , there are two values of ψ that satisfy this condition. When $M_{3R} = M_2 = 1.0$ and $\gamma = 1.3$, they are 1.072 and -0.82 , the former obviously being the one that appears in Fig. 9.75 and the latter having no practical use. For $M_{3R} = M_2 = 1.2$ and $\gamma = 1.3$, they are 1.102 and -0.746 . The physical meaning of this convenient convergence is clear enough, namely, that near $M_{3R} = M_2$, where the stator and rotor airfoil exit conditions are similar, the stage loading parameter ψ must be near unity regardless of the other stage parameters.

9.5.6.2 Multistage turbine design. When the required stage loading coefficient ψ for a design is greater than 2.0, a single-stage design would require a hopeless negative reaction [Eq. (9.87)] and would be impossible to design with high aerodynamic efficiency. A desirable multistage design would have the total temperature difference distributed evenly among the stages:

$$(\Delta T_t)_{\text{turbine}} = (\text{number of stages}) \times (\Delta T_t)_{\text{stage}}$$

This would result in stages with the same stage loading coefficients [Eq. (9.20)] and same degree of reaction [Eq. (9.87)] for the same rotor speed U . For a three-stage design, we get

$$\psi_{s1} = \psi_{s2} = \psi_{s3} \quad \text{and} \quad (^o R_t)_{s1} = (^o R_t)_{s2} = (^o R_t)_{s3}$$

To obtain the choked flow in the first-stage stator (nozzle), the Mach number entering the rotor M_2 is slightly supersonic. The Mach numbers in the remaining stages are kept subsonic. The net result is that the stage loading of the first stage is larger than the loading of any of the other stages. For a three-stage design, the

stage loading coefficient and degree of reaction of the second and third stages are nearly equal.

9.5.7 Shaft Speed

The design rotational speed of a spool (shaft) having stages of compression driven by a turbine is initially determined by that component that limits the speed because of high stresses. For a low-pressure spool, the first stage of compression, since it has the greatest AN^2 , normally dictates the rotational speed. The first stage of turbine on the high-pressure spool normally determines that spool's rotational speed because of its high AN^2 or high disk rim speed at elevated temperature.

9.5.8 Design Process

The design process requires both engineering judgment and knowledge of typical design values. Table 9.18a gives the range of design parameters for axial-flow turbines that can be used for guidance. The comparison of turbines for Pratt & Whitney engines in Table 9.18b shows typical turbine design values and the leading trends in turbine technology. Note the increases over the years in inlet temperature, mass flow rate, and output power.

From Table 9.18b, comparison of the JT3D and JT9D high-pressure turbines shows that the stage loading coefficient did not appreciably change between the designs. However, the turbine inlet temperature increased to a value above the working temperature of available materials, requiring extensive use of cooling air. The stage loading coefficient for the low-pressure turbine increased dramatically, reducing the number of stages to four. If the stage loading coefficient of the low-pressure turbine of the JT3D were not increased significantly in the design of the JT9D, about six or seven stages of low-pressure turbine would have been required—increasing both cost and weight.

Table 9.18a Range of axial-flow turbine design parameters

Parameter	Design range
High-pressure turbine	
Maximum AN^2	$4-5 \times 10^{10} \text{ in.}^2 \cdot \text{rpm}^2$
Stage loading coefficient	1.4–2.0
Exit Mach number	0.40–0.50
Exit swirl angle, deg	0–20
Low-pressure turbine	
Inlet corrected mass flow rate	40–44 $\text{lbf}/(\text{s} \cdot \text{ft}^2)$
Hub/tip ratio at inlet	0.35–0.50
Maximum stage loading at hub	2.4
Exit Mach number	0.40–0.50
Exit swirl angle, deg	0–20

Table 9.18b Comparison of Pratt & Whitney engines

Parameter	JT3D	JT9D
Year of introduction	1961	1970
Engine bypass ratio	1.45	4.86
Engine overall pressure ratio	13.6	24.5
Core engine flow, lb/s	187.7	272.0
High-pressure turbine		
Inlet temperature, °F	1745	2500
Power output, hp	24,100	71,700
Number of stages	1	2
Average stage loading coefficient	1.72	1.76
Coolant plus leakage flow, %	2.5	16.1
Low-pressure turbine		
inlet temperature, °F	1410	1600
Power output, hp	31,800	61,050
Number of stages	3	4
Average stage loading coefficient	1.44	2.47
Coolant plus leakage flow, %	0.7	1.4

9.5.8.1 Steps of design. The material presented in previous sections can now be applied to the design of an axial-flow turbine. The complete design process for a turbine will include the following items:

- 1) Selection of rotational speed and annulus dimensions
- 2) Selection of the number of stages
- 3) Calculation of airflow angles for each stage at the mean radius
- 4) Calculation of airflow angle variations from the hub to tip for each stage
- 5) Selection of blade material
- 6) Selection of blading using experimental cascade data
- 7) Selection of turbine cooling, if needed
- 8) Verification of turbine efficiency based on cascade loss data
- 9) Prediction of off-design performance
- 10) Rig testing of design

Items 1–5 will be covered in this section. The other steps are covered in Refs. 42, 43, 22, and 29. The design process is inherently iterative, often requiring the return to an earlier step when prior assumptions are found to be invalid. Many technical specialties are interwoven in a design, e.g., an axial-flow turbine involves at least thermodynamics, aerodynamics, structures, materials, heat transfer, and manufacturing processes. Design requires the active participation and disciplined communication by many technical specialists.

Example 9.14

We will consider the design of a turbine suitable to power the eight-stage, axial-flow compressor designed earlier in this chapter for a simple turbojet gas turbine

engine (see Example 9.7). From engine cycle and compressor design calculations, a suitable design point for the turbine of such an engine at sea-level, standard-day conditions ($P = 14.696$ psia and $T = 518.7^\circ\text{R}$) may emerge as follows:

Compressor pressure ratio: 10.41	Rotor speed ω : 800 rad/s
Compressor flow rate: 150 lbm/s	Turbine flow rate: 156 lbm/s
Compressor efficiency: 86.3%	T_t entering turbine: 3200°R
Compressor exit T_e : 1086°R	P_t entering turbine: 143.1 psia
Compressor γ : 1.4	Turbine γ : 1.3
Compressor R : $53.34 \text{ ft} \cdot \text{lbf}/(\text{lbf} \cdot {}^\circ\text{R})$	Turbine R : $53.40 \text{ ft} \cdot \text{lbf}/(\text{lbf} \cdot {}^\circ\text{R})$

From these specified data, we now investigate the aerodynamic design of an axial-flow turbine.

The compressor input power is

$$\dot{W}_c = \dot{m}c_p(T_{te} - T_{ti}) = (150 \times 0.240)(1086 - 518.7) = 20,423 \text{ Btu/s}$$

$$= 21.55 \text{ MW}$$

Assuming that the compressor input power is 0.98 of the turbine output power (the other 2% of turbine power goes to shaft takeoff power and bearing losses), the required output power of the turbine is 22.0 MW (21.55 MW/0.98). The total temperature leaving the turbine is

$$T_{tc} = T_{ti} - \frac{\dot{W}_t}{\dot{m}c_p} = 3200 - \frac{22,000/1.055}{156 \times 0.297} = 3200 - 450.1 = 2749.9^\circ\text{R}$$

The turbine temperature ratio ($\tau_t = T_{te}/T_{ti}$) is 0.8593. If the flow entering the rotor has a Mach number of 1.2 at 60 deg to the centerline of the turbine and a 1% total pressure loss through the turbine stator (nozzle), the annulus area entering the rotor is

$$A_2 = \frac{\dot{m}\sqrt{T_{t2}}}{(\cos \alpha_2)(P_{t2})\text{MFP}(M_2)}$$

$$= \frac{156\sqrt{3200}}{\cos 60 \text{ deg} \times 143.1 \times 0.99 \times 0.502075\sqrt{53.34/53.40}} = 248.3 \text{ in.}^2$$

For a rotor angular speed ω of 800 rad/s, AN^2 for the rotor is 1.45×10^{10} in.²·rpm²—this blade stress is within the capability of modern cooled turbine materials (about 2 to 3×10^{10} in.²·rpm²).

Calculation of the stage loading coefficient for the turbine helps in determining the number of turbine stages. For the turbine mean radius equal to that of the compressor, the stage loading coefficient on the mean line is

$$\psi = \frac{g_c c_p \Delta T_t}{(\omega r_m)^2} = \frac{7455 \times 450.1}{(800 \times 17.04/12)^2} = 2.600$$

Using Fig. 9.73, we see that this value of stage loading coefficient is larger than that possible for a single-stage turbine. Either the mean rotor speed ωr_m must be

Table 9.19 Variation of stage loading, radii, and rim speed with mean radius for Example 9.14 single-stage design

r_m , in.	ψ	r_t , in.	r_h , in.	r_h/r_t	U_r , ft/s
16.00	2.949	17.23	14.77	0.857	918
17.04	2.600	18.20	15.88	0.873	992
18.00	2.330	19.10	16.90	0.885	1060
19.00	2.091	20.04	17.96	0.896	1131
20.00	1.887	20.99	19.01	0.906	1201
21.00	1.712	21.94	20.06	0.914	1271

increased to reduce the stage loading coefficient for a single-stage turbine, or a two-stage turbine will be required. Because increasing the rotor angular speed ω will increase the blade stress AN^2 and because only a little margin exists, we will investigate the effect of increasing the mean radius on stage loading coefficient, annulus radii (r_t and r_h), and rim speed (U_r —assuming the rim radius is 1 in. smaller than that of the hub). From the results given in Table 9.19, we can see that a single-stage turbine would require a mean radius of 19 to 20 in. to reduce the stage loading coefficient and keep the rim speed below about 1200 ft/s. This would result in a tip radius equal to or larger than the compressor's inlet radius. In addition, the tip radius of 20 to 21 in. is much larger than current turbines for gas turbine engines that range between 10 and 17 in. Although a single-stage turbine is desirable because of the reduced weight, the low rotor angular speed of 800 rad/s makes this size undesirable.

For a smaller turbine, the designer might consider increasing the rotor angular speed and redesigning the compressor. A rotor angular speed of 1000 rad/s for a turbine with a 16-in. mean radius has a stage loading coefficient for the mean radius of 1.885 and a rim speed of 1148 ft/s, which is possible for a single stage.

The designs of both a single-stage turbine and a two-stage turbine are performed in the following sections. The computer program TURBN is used to ease the calculational burden in both designs.

9.5.8.2 Single-stage design. We consider a single-stage turbine with the following characteristics:

Rotor angular speed ω : 800 rad/s	Turbine mass flow rate: 156 lbm/s
T_t entering turbine: 3200°R	P_t entering turbine: 143.1 psia
T_t leaving turbine: 2749.1°R	Ratio of specific heats: 1.3

To keep the degree of reaction at the hub from being too negative at a reasonable value of the stage loading coefficient ψ , we consider a nonzero exit swirl angle α_3 for a stage with a hub speed of about 1200 ft/s (this corresponds to a rim speed of about 1130 ft/s, which will limit the disk stress). This hub speed corresponds to a hub radius of 18 in. and a tip radius of about 20.1 in. The

computer program TURBN was run with the exit swirl angle α_3 unknown, the data just listed, and the following additional input data:

Mean rotor speed ω_r : 1270 ft/s	ω : 800 rad/s
M_2 : 1.1	α_2 : 60 deg
M_1 : 0.4	α_1 : 0 deg
u_3/u_2 : 1.0	$\phi_{t\text{stator}} = 0.06$ and $\phi_{t\text{rotor}} = 0.15$
Z_s : 0.9	$(c/h)_s$: 1.0
Z_r : 0.9	$(c/h)_r$: 1.0

Computer calculations yield the single-stage turbine summarized in Table 9.20 with hub and tip tangential velocities based on free-vortex swirl distribution. This is a viable single-stage design with moderate exit swirl α_3 , positive reaction, and subsonic M_{3R} at the tip.

This design gives a blade AN^2 of 1.44×10^{10} in.²·rpm² and hub speed of 1201 ft/s. This AN^2 value is well within the limits of cooled turbine materials, and the low hub speed is below the limiting speed of turbine disk materials.

A cross-sectional sketch of the single-stage turbine just designed and plotted by the computer program TURBN is shown in Fig. 9.76. Note that this sketch does not show the required exit guide vanes that will turn the flow back to axial. The estimated axial length L shown in Fig. 9.76 is based on the input values of Z and c/h for the stator and rotor blades and the scaling relationships of Fig. 9.69. For the input values of Z and c/h , the resulting solidity at the mean radius, number of blades, and chord length for the stator and rotor are as shown in Table 9.21.

The selected axial chord and number of blades for the stator or rotor depend on many factors (e.g., flow through the blades, vibration, blade attachment). Figure 9.77 shows the computer sketch of the blades at the mean radius, using C4 base profiles.

9.5.8.3 Two-stage design. In a two-stage design, the stage loading coefficients ψ are lower and the temperature ratios τ_s are higher than those for a single-stage design. This results in higher reactions, less turning of the flow, and lower loss coefficients. For good flow control of the turbine, the first-stage stator (nozzle) should be choked, which requires that M_2 for this stage be supersonic. Inspection of Fig. 9.75 shows that at low ψ and high τ_s , the value of M_{3R} is a little less than M_2 —thus, we will want to select a low supersonic value of M_2 (about 1.05) for the first stage. A balanced design would have about the same α_2 values for both stages with the first-stage M_{3R} below 0.9.

The two-stage turbine will be designed with a 17.04-in. mean radius (same as multistage compressor) at an rpm of 7640 ($\omega = 800$ rad/s), giving a mean rotor speed $U_m = \omega r_m$ of 1136 ft/s. An initial starting point for the design of this two-stage turbine is constant axial velocity through the rotor ($u_3 = u_2$), zero exit swirl ($\alpha_3 = 0$), and a second-stage M_2 of 0.7. The stage loading coefficients and other flow properties depend on the split in temperature drop between the stages. Calculations were performed by using the computer program TURBN.

Table 9.20 Results for Example 9.14 single-stage axial-flow turbine design

Property	Station						
	1 <i>h</i>	1 <i>m</i>	1 <i>f</i>	2 <i>h</i>	2 <i>m</i>	2 <i>t</i>	2 <i>Rm</i>
T_1	3200	3200	3200	3200	3200	3200	2909
T	3125	3125	3125	2665	2708	2745	2708
P_t	psia	143.1	143.1	138.8	138.8	138.8	91.8
P	psia	129.1	129.1	62.8	67.4	71.5	67.4
M	0.400	0.400	0.400	1.157	1.100	1.051	0.702
V	ft/s	1057	1057	2823	2705	2602	1727
u	ft/s	1057	1057	0	1353	1353	1353
v	ft/s	0	0	2477	2343	2222	1073
α	deg	0	0	61.36	60.00	58.67	—
β	deg	—	—	—	—	38.42	49.17
Radii	in.	18.25	19.05	19.85	18.02	19.05	20.08
Hub:	R_t	0.0990	$A_1 = 190.78 \text{ in.}^2$	$A_1 = 190.78 \text{ in.}^2$	$A_2 = 247.52 \text{ in.}^2$	$\pi_s = 0.4770$	$\psi = 2.0776$
Mean:	R_t	0.1939	$A_2 = 247.52 \text{ in.}^2$	$A_2 = 247.52 \text{ in.}^2$	$A_3 = 291.11 \text{ in.}^2$	$M_{3Rt} = 0.875$	$\Phi = 1.0652$
Tip:	R_t	0.2746	$A_3 = 291.11 \text{ in.}^2$	$A_3 = 291.11 \text{ in.}^2$	$\eta_s = 89.57\%$	$\tau_s = 0.8593$	$\pi_s = 0.4770$
							$\pi_s = 0.4770$
							$\psi = 2.0776$
							$\Phi = 1.0652$
							$AN^2 \text{ at } 2 = 1.44 \times 10^{10} \text{ in.}^2 \cdot \text{rpm}^2$

Size [in]
Front
 $r_h = 18.25$
 $r_t = 19.85$
Back
 $r_h = 17.84$
 $r_t = 20.26$

L = 4.88 in

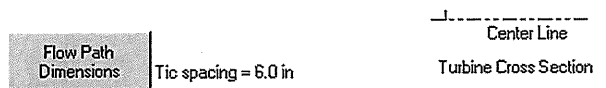


Fig. 9.76 Sketch of cross section for single-stage turbine design.

with α_2 unknown at different values of the temperature leaving the first-stage turbine. The resulting α_2 and M_{3Rt} values are listed in Table 9.22. An interstage temperature of 2925°R gives a balance design for α_2 values with the first stage M_{3Rt} , above 0.9. The value of M_{3Rt} can be reduced by selecting a value for the axial velocity ratio u_3/u_2 less than unity.

A design with an interstage temperature of 2925°R and first-stage u_3/u_2 of 0.9 is selected to reduce M_{3Rt} . The losses for the first stage and second stage are estimated by using polytropic efficiencies of 0.9 and 0.92, respectively, and stator loss coefficients of 0.06 and 0.02, respectively. For all blades, a value of 0.9 is used for the tangential force coefficient Z, and a value of 1.0 is used for the chord/height ratio c/h . Results for both stages are presented in Tables 9.23

Table 9.21 Blade results for single-stage turbine

Solidity	Number of blades	Chord, in.
Stator	0.979	64
Rotor	1.936	103

Stage: 1	Nozzle	Rotor
Inlet	00.0	38.4
Exit	68.7	57.3
Thickness	12.0%	12.0%
Profile:	T6	T6
Chord (in)	1.826	2.234

Radial Position 50% hub/tip

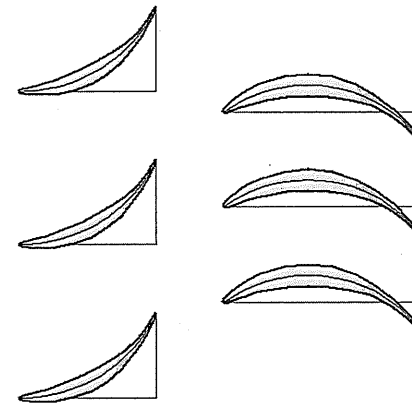
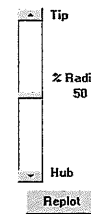


Fig. 9.77 Sketch of blades for single-stage turbine design.

and 9.24 with hub and tip tangential velocities based on free-vortex swirl distribution.

A cross-sectional sketch of the two-stage turbine just designed and plotted by TURBN is shown in Fig. 9.78. The sketch shows the stator and rotor for both stages. Note that the turbine exit stator is not shown in the sketch. For the input values of Z and c/h , the resulting solidity at the mean radius, number of blades, and chord length for the stator and rotor blades of the two stages are as shown in Table 9.25.

The selected axial chord and number of blades for the stator and rotor depend on many factors (e.g., flow through the blades, vibration, blade attachment). Figures 9.79 and 9.80 show the computer sketch of the blades at the mean radius, using C4 base profiles for the first and second stages, respectively.

Table 9.22 Variation of stage parameters with interstage temperature for Example 9.14 two-stage design

T_B , $^{\circ}\text{R}$	ψ	τ_s	Stage 1		Stage 2		
			α_2 , deg	M_{3Rt}	ψ	τ_s	α_2 , deg
2875	1.8750	0.8984	55.0	0.7774	1.0034	0.9565	28.61
2900	1.7307	0.9063	49.12	0.8467	0.8659	0.9482	34.90
2925	1.5865	0.9141	43.88	0.9068	1.0102	0.9401	41.65
2950	1.4423	0.9219	39.06	0.9587	1.1544	0.9322	49.13
2975	1.2981	0.9297	34.55	1.0034	1.2986	0.9243	57.90

Table 9.23 Results for Example 9.14, first stage of two-stage axial-flow turbine design

Property	Station					
	1h	1m	1t	2h	2m	2t
T_t	3200	3200	3200	3200	3200	3012
T	3125	3135	3125	2746	2746	2734
P_t	143.1	143.1	143.1	139.1	139.1	106.9
P	psia	129.1	129.1	69.2	71.6	71.6
M	0.400	0.400	0.400	1.079	1.050	1.024
V	ft/s	1057	1057	2662	2660	2545
u	ft/s	1057	1057	1874	1874	1874
v	ft/s	0	0	1891	1802	1722
α	deg	0	0	45.25	43.88	42.57
β	deg	—	—	—	—	—
Radii	in.	16.15	17.04	17.93	16.24	17.04
Hub:	$^oR_t = 0.0359$	$A_1 = 190.78 \text{ in.}^2$				
Mean:	$^oR_t = 0.0437$	$A_2 = 170.34 \text{ in.}^2$				
Tip:	$^oR_t = 0.1129$	$A_3 = 194.88 \text{ in.}^2$				
			$M_{3Rt} = 0.8370$	$\tau_s = 0.9141$	$\pi_s = 0.6488$	$\psi = 1.5865$
			$\eta_s = 90.44\%$	AN^2 at 2 = 9.94	AN^2 at 2 = 9.94 $\times 10^{10} \text{ in.}^2 \cdot \text{rpm}^2$	$\Phi = 1.650$

Table 9.24 Results for Example 9.14 second stage of two-stage axial-flow turbine design

Property	Station					
	1h	1m	1t	2h	2m	2t
T_t	2925	2925	2925	2925	2925	2837
T	2734	2734	2734	2725	2725	2638
P_t	92.84	92.84	92.84	92.35	92.35	80.85
P	psia	69.27	69.27	66.41	67.92	69.15
M	0.683	0.683	0.683	0.726	0.700	0.678
V	ft/s	1687	1687	1786	1727	1677
u	ft/s	1687	1687	1687	1290	1290
v	ft/s	0	0	1235	1148	1072
α	deg	0	0	43.75	41.65	39.71
β	deg	—	—	—	—	—
Radii	in.	16.13	17.04	17.95	15.83	17.04
Hub:	$^oR_t = 0.4148$	$A_1 = 194.88 \text{ in.}^2$				
Mean:	$^oR_t = 0.4949$	$A_2 = 258.99 \text{ in.}^2$				
Tip:	$^oR_t = 0.5596$	$A_3 = 293.69 \text{ in.}^2$				
			$M_{3Rt} = 0.7337$	$\tau_s = 0.9401$	$\pi_s = 0.7477$	$\psi = 1.0102$
			$\eta_s = 92.24\%$	AN^2 at 2 = 92.24% $\times 10^{10} \text{ in.}^2 \cdot \text{rpm}^2$	AN^2 at 2 = 92.24% $\times 10^{10} \text{ in.}^2 \cdot \text{rpm}^2$	$\Phi = 1.136$

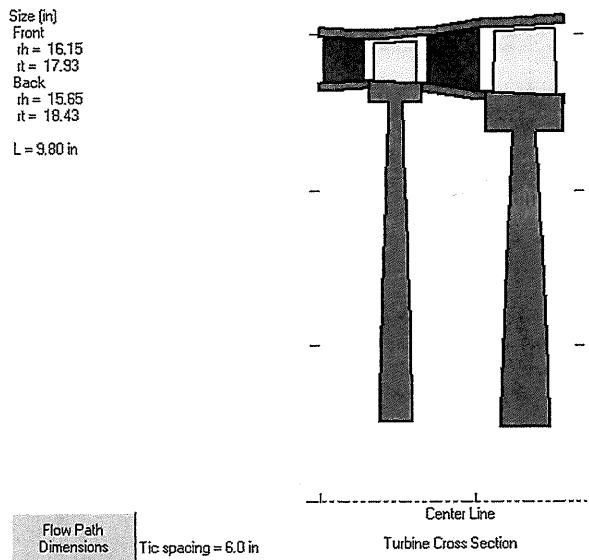


Fig. 9.78 Sketch of cross section for two-stage turbine design.

For the first stage, this design gives a blade AN^2 of $9.94 \times 10^9 \text{ in.}^2 \cdot \text{rpm}^2$ and disk speed of about 1020 ft/s. This AN^2 is well within the limits of cooled turbine materials, and the low rim speed is below the limiting speed of turbine disk materials.

9.5.9 Turbine Cooling

The turbine components are subjected to much higher temperatures in the modern gas turbine engines being designed and built today than was possible 60 years ago. This is due mainly to improvements in metallurgy and cooling of turbine components. The cooling air to cool the turbine is bleed air from the compressor. A schematic of a typical turbine cooling system is shown in

Table 9.25 Blade results for two-stage turbine

	Stage 1		Stage 2	
	Stator	Rotor	Stator	Rotor
Solidity	0.725	1.880	1.643	1.254
Blades	46	118	83	52
Chord, in.	1.686	1.706	2.120	2.581

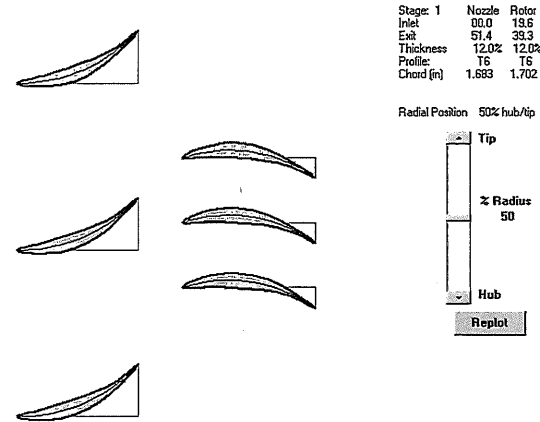


Fig. 9.79 Sketch of blades for first stage of two-stage turbine design.

Fig. 9.81. The stator blades and the outer wall of the turbine flow passage use cooling air that travels from the compressor between the combustor and outer engine case. The turbine rotor blades, disks, and inner wall of the turbine flow passage use cooling air that is routed through inner passageways.

The first-stage stator blades (nozzles) are exposed to the highest turbine temperatures (including the hot spots from the combustor). The first-stage rotor blades are exposed to a somewhat lower temperature because of circumferential averaging, dilution of turbine gases with first-stage stator cooling air, and relative

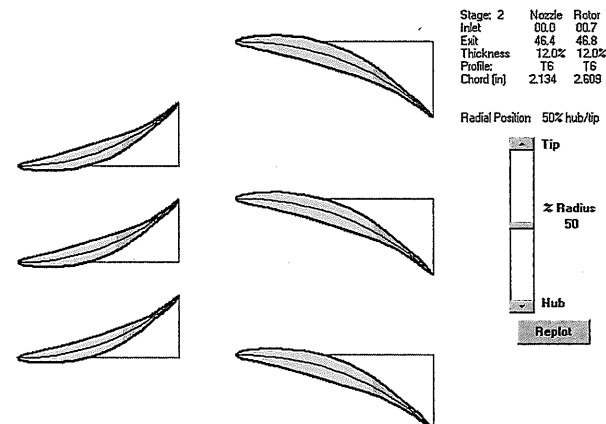


Fig. 9.80 Sketch of blades for second stage of two-stage turbine design.

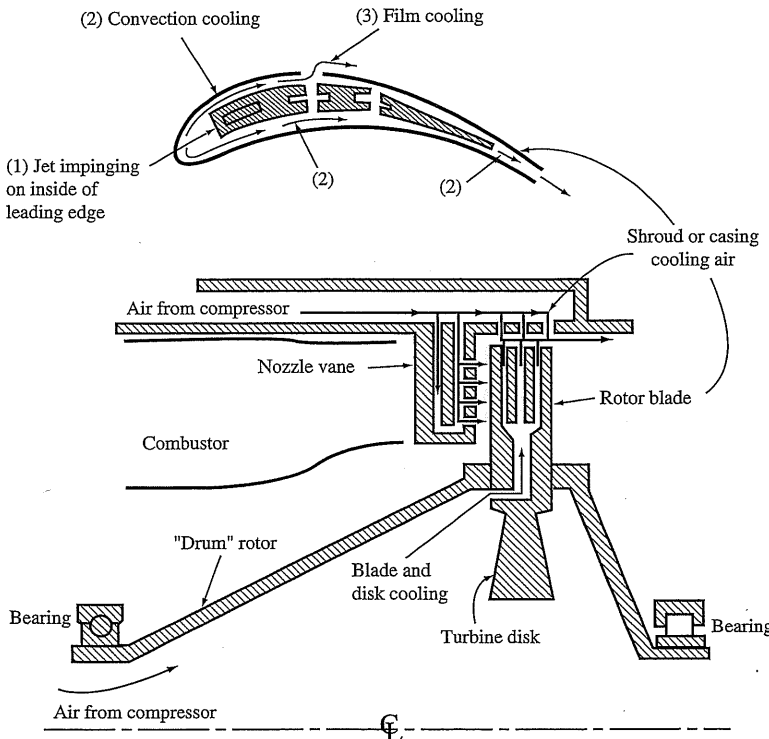


Fig. 9.81 Schematic of air-cooled turbine (from Ref. 28).

velocity effects. The second-stage stator blades are exposed to an even lower temperature because of additional cooling air dilution and power extraction from the turbine gases. The turbine temperature decreases in a like manner through each blade row.

The cooling methods used in the turbine are illustrated in Fig. 9.82 and can be divided into the following categories:

- 1) Convection cooling
- 2) Impingement cooling
- 3) Film cooling
- 4) Full-coverage film cooling
- 5) Transpiration cooling

Applications of these five methods of cooling to turbine blades are shown in Fig. 9.83.

Figure 9.84 shows a typical first-stage stator (nozzle) blade with cooling. This stator has cooling holes along its nose (leading edge) and pressure surface (gill

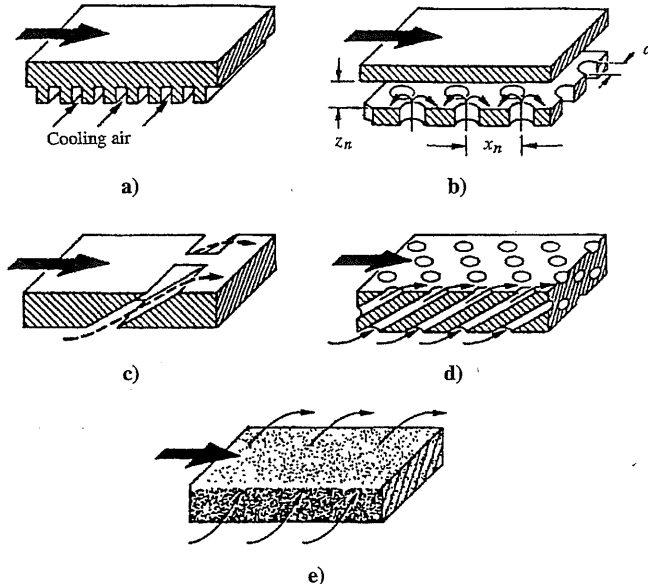


Fig. 9.82 Methods of turbine cooling (Ref. 42): a) convection cooling, b) impingement cooling, c) film cooling, d) full-coverage film cooling, e) transpiration cooling.

holes) in addition to cooling flow exiting at its trailing edge. The cooling holes on the inside wall are also shown.

A rotor blade of the General Electric CF6-50 engine is shown in Fig. 9.85. The cross section of the blade shows the elaborate internal cooling and flow exiting the blade tip (through its cap) and along the trailing edge. The blade isometric shows flow through the gill holes on the pressure surface in addition to the tip and trailing-edge cooling flows.

9.5.10 Turbine Performance

The flow enters a turbine through stationary airfoils (often called *stator blades* or *nozzles*) that turn and accelerate the fluid, increasing its tangential momentum. Then the flow passes through rotating airfoils (called *rotor blades*) that remove energy from the fluid as they change its tangential momentum. Successive pairs of stationary airfoils followed by rotating airfoils remove additional energy from the fluid. To obtain high output power to weight from a turbine, the flow entering the first-stage turbine rotor is normally supersonic, which requires the flow to pass through sonic conditions at the minimum passage area in the first-stage stators (nozzles). From Eq. (8.3), the corrected inlet mass flow rate based on this minimum passage area (throat) will be constant for fixed-inlet-area turbines. This flow characteristic is shown in the typical turbine flow map (Fig. 9.86) when the expansion ratio across the turbine (ratio

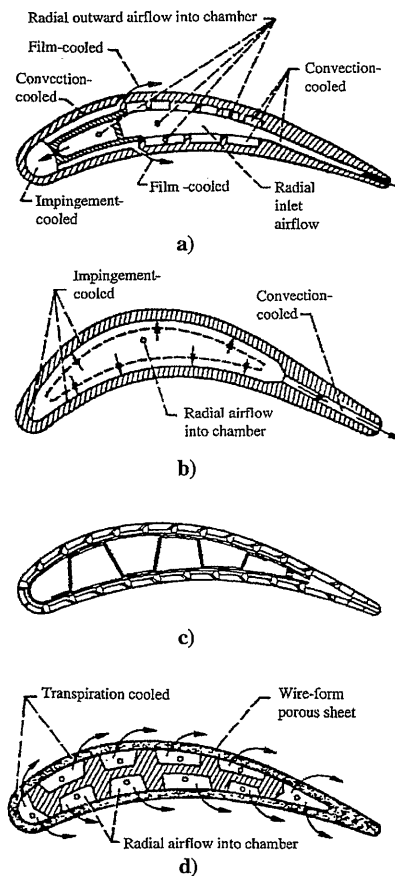


Fig. 9.83 Turbine blade cooling (Ref. 42): a) convection-, impingement-, and film-cooled blade configuration, b) convection- and impingement-cooled blade configuration, c) full-coverage film-cooled blade configuration, d) transpiration-cooled blade configuration.

of total pressure at exit to total pressure at entrance $P_{t4}/P_{t5} = 1/\pi_t$ is greater than about 2 and the flow at the throat is choked.

The performance of a turbine is normally shown by using the total pressure ratio, corrected mass flow rate, corrected turbine speed, and component efficiency. This performance is presented in either two maps or one consolidated map. One map shows the interrelationship of the total pressure ratio, corrected mass flow rate, and corrected turbine speed, like that depicted in Fig. 9.86 for a single-stage turbine. Because the corrected-speed lines collapse into one line when the turbine is choked, the turbine efficiency must be shown in a

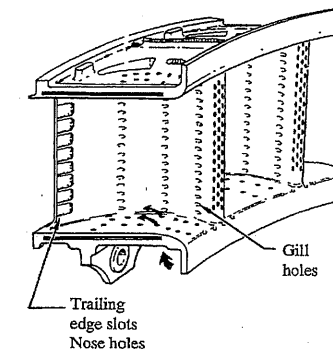


Fig. 9.84 Typical cooled turbine nozzle. (Courtesy of General Electric.)

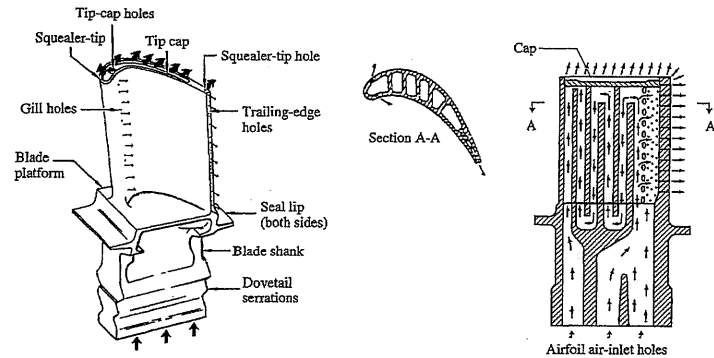


Fig. 9.85 Construction features of air-cooled turbine blade. (Courtesy of General Electric.)

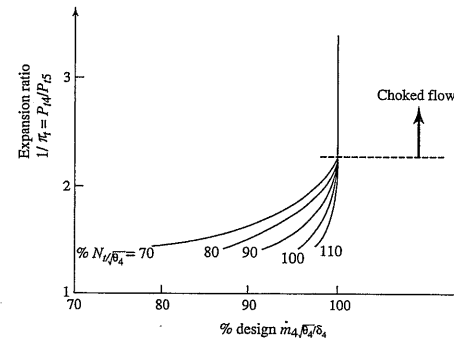


Fig. 9.86 Typical turbine flow map.

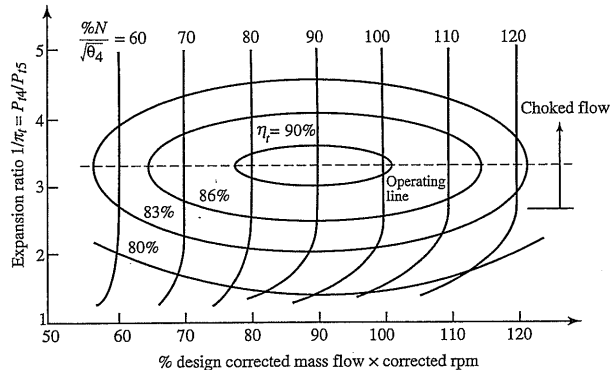


Fig. 9.87 Typical turbine consolidated performance map.

separate map (see Fig. 8.5b). The constant corrected speed lines of Fig. 9.86 can be spread out horizontally by multiplying the corrected mass flow rate by the percentage of corrected speed. Now the turbine efficiency lines can be superimposed without cluttering the resulting performance map. Figure 9.87 shows the consolidated turbine performance map of a multistage turbine with all four performance parameters: total pressure ratio, corrected mass flow rate, corrected turbine speed, and efficiency.

For the majority of aircraft gas turbine engine operation, the turbine expansion ratio is constant and the turbine operating line can be drawn as a horizontal line in Fig. 9.87 (it would collapse to an operating point on the flow map of Fig. 9.86). At off-design conditions, the corrected speed and efficiency of a turbine change very little from their design values. In the analysis of gas turbine engine performance of Chapter 8, we considered that the turbine efficiency was constant.

9.6 Centrifugal-Flow Turbine Analysis

The flow through the stators (nozzles) and rotor of a centrifugal flow turbine is shown in Fig. 9.88. The stators accelerate the flow and increase its tangential velocity. The rotor decreases the tangential velocity of the flow as it removes energy from the flow. Flow exiting the rotor is normally axial, but some tangential (swirl) velocity may still be present. This type of turbine was used in the turbojet engine of von Ohain and is used extensively in turbochargers and very small gas turbine engines.

Figure 9.89 shows the station numbering used in the analysis of the centrifugal-flow turbine. The flow enters the stators at station 1 and leaves at station 2. It then passes through the rotor and leaves at station 3. Normally the flow leaving the rotor is axial ($V_3 = u_3$). Application of the Euler turbine equation to the flow through the stator and rotor, assuming adiabatic stator, gives

$$h_{t1} - h_{t3} = \frac{U_t v_2}{g_c} \quad (9.126)$$